AD NUMBER

ADA196789

NEW LIMITATION CHANGE

TO

Approved for public release, distribution unlimited

FROM

Distribution authorized to U.S. Gov't. agencies and their contractors; Administrative/Operational use; 7 Jult 1988. Other requests shall be referred to Office Of Naval Research, Arlington, VA 22217-5000.

AUTHORITY

ONR ltr dtd 27 Jul 1988

I-ARA-88-U-24

(4)

BEAM HANDLING AND EMITTANCE CONTROL

J. R. Thompson
M. L. Sloan
B. N. Moore
J. R. Uglum

Austin Research Associates
1901 Rutland Drive
Austin, Texas 78758

7 July 1988

Technical Report

CONTRACT NO. ONR N00014-86-C-0568

Funding Provided by

Strategic Defense Initiative Organization/
Innovative Science and Technology Office

Prepared for:

Office of Naval Research
Washington, DC

AD-A196 289

REPORT DOCUMENTATION PAGE

Form Approved
OMB No. 0704-0188

1a. REPORT SECURITY CLASSIFICATION UNCLASSIFIED	1b. RESTRICTIVE MARKINGS
2a. SECURITY CLASSIFICATION AUTHORITY N/A since Unclassified	3. DISTRIBUTION/AVAILABILITY OF REPORT
2b. DECLASSIFICATION/DOWNGRADING SCHEDULE N/A since Unclassified	
4. PERFORMING ORGANIZATION REPORT NUMBER(S) I-ARA-88-U-24	5. MONITORING ORGANIZATION REPORT NUMBER(S)
6a. NAME OF PERFORMING ORGANIZATION Austin Research Associates 6b. OFFICE SYMBOL (If applicable)	7a. NAME OF MONITORING ORGANIZATION Office of Naval Research
6c. ADDRESS (City, State, and ZIP Code) 1901 Rutland Drive Austin, Texas 78758	7b. ADDRESS (City, State, and ZIP Code) Arlington, VA 22217-5000
8a. NAME OF FUNDING/SPONSORING ORGANIZATION Strategic Defense Initiative Organization 8b. OFFICE SYMBOL (If applicable) SDIO/IST	9. PROCUREMENT INSTRUMENT IDENTIFICATION NUMBER N00014-86-C-0568
8c. ADDRESS (City, State, and ZIP Code) Washington, DC 20301	10. SOURCE OF FUNDING NUMBERS PROGRAM ELEMENT NO. / PROJECT NO. / TASK NO / WORK UNIT ACCESSION NO.

11. TITLE (Include Security Classification)

BEAM HANDLING AND EMITTANCE CONTROL (U)

12. PERSONAL AUTHOR(S)
Thompson, J. R.; Sloan, M. L.; Moore, B. N.; Uglum, J. R.

13a. TYPE OF REPORT	13b. TIME COVERED	14. DATE OF REPORT (Year, Month, Day)	15. PAGE COUNT
Technical	FROM 860901 TO 880228	880715	66

16. SUPPLEMENTARY NOTATION

17. COSATI CODES			18. SUBJECT TERMS (Continue on reverse if necessary and identify by block number)
FIELD	GROUP	SUB-GROUP	Beam Brightness, Beam Transport, Emittance Control, Image Charge Fields, Beam Quality

19. ABSTRACT (Continue on reverse if necessary and identify by block number)

This report reviews the results of calculations which concern techniques of beam handling and emittance control for high current beams in advanced accelerators. Beam quality requirements for acceptable performance of beam-driven free electron laser devices for SDI missions are examined. The beam quality achievable in high current, space-charge-limited diodes is reviewed and found to be potentially high. Emittance growth during gas-focused transport due to streaming instabilities between beam electrons and gas ions is briefly examined, and estimated to be modest. The principal threat to beam quality degradation is estimated to occur during the lengthy process of acceleration and transport past protuberances, constrictions, or discontinuities in the waveguide wall, or during beam aperturing. A Hamiltonian-theoretic analysis of emittance growth during high current electron beam transport, coupled with an envelope equation analysis of the induced transverse beam oscillations, is applied to develop scaling

20. DISTRIBUTION/AVAILABILITY OF ABSTRACT ☐ UNCLASSIFIED/UNLIMITED ☒ SAME AS RPT. ☐ DTIC USERS	21. ABSTRACT SECURITY CLASSIFICATION UNCLASSIFIED
22a. NAME OF RESPONSIBLE INDIVIDUAL	22b. TELEPHONE (Include Area Code) / 22c. OFFICE SYMBOL

19. ABSTRACT (Continued)

laws for the emittance growth suffered during such events as beam acceleration, propagation past irises or constrictions in the waveguide wall, beam aperturing, and axial variation in the magnetic guide field strength. Criteria are developed for preventing excessive emittance growth by avoiding abrupt axial variations and providing sufficiently strong focusing forces. Designed variations in the waveguide wall shape and in the strength of the magnetic guide field may be introduced to greatly reduce emittance growth during such events as beam acceleration.

Keywords: Energy; Defense Initiative; Microfiche 18

TABLE OF CONTENTS

LIST OF ILLUSTRATIONS

I. INTRODUCTION

This document comprises a technical report of research conducted by Austin Research Associates under ONR Contract N00014-86-C-0568 during the period 1 September 1986 through 28 February 1988 on the subject of beam handling and emittance control in advanced accelerators. The motivation for this research is described in Section II, which includes an overview of the relevance of this research to other ongoing research efforts in the development of free-electron lasers for SDI missions. Section III contains a review of our research progress on the four specific technical tasks undertaken during this 18-month period of performance. Technical references for this report are listed in Section IV.

Our primary efforts under this contract were devoted to techniques of emittance control of beams extracted from field-immersed cathodes and transported through an accelerator with solenoidal magnetic focusing. This work has been documented in a recent paper [Ref. 3] which is included herein as Appendix A.

Research on these subjects is continuing under renewal funding of this contract.

II. FEL BEAM QUALITY REQUIREMENTS

Advanced electron accelerators will emphasize high current (1 kA or more) concepts that can be scaled to energies of a few hundred megavolts--capabilities which are beyond anything now in existence. As such accelerators are developed, the evolution toward higher currents, higher particle energy, and higher acceleration gradients all conspire to make it more difficult to preserve the necessary beam quality and brightness (i.e., low emittance and energy spread at high current). Although good beam quality is necessary for acceptable performance of almost all beam-driven SDI applications, the beam quality requirements are particularly stringent for free-electron laser (FEL) devices, where to the extent possible all electrons should have the same axial velocity $\beta_z c$, matched for optimum growth of the FEL signal.

The goal of our own ongoing research on beam quality control in accelerators has always been to obtain beam transport designs which are compatible with these stringent beam quality requirements posed by FEL applications. Building upon other in-house FEL research, we have explored in some detail the specific FEL performance benefits which follow from good beam quality, and which imply the FEL beam quality requirements. These FEL performance considerations, and the performance versus beam quality scaling laws which result, are outlined in the remainder of this section.

The recently published APS Study: Science and Technology of directed Energy Weapons [Ref. 1] may be used to define the operating parameters of a "standard" SDI FEL system. It is estimated therein that for strategic defense applications, a ground-based free electron laser should produce an average power level of at least 1 GW at 1 μm wavelength, corresponding to peak laser powers of 0.1-1.0 TW. The near optical wavelength requirement, together with technological constraints which limit the wiggler wavelength above a few cm, implies the need for particle energy in excess of 100 MeV--and typically several hundred MeV. The peak laser power requirement, together with some loss of efficiency in conversion of electron beam energy into laser energy, then implies the need for peak electron current in excess of 1 kA--and typically several kA. In this parameter range of energy and current, the FEL will operate in the single particle Compton regime for which the collective space charge fields are unimportant. However, in this regime both beam quality and beam brightness are "vital issues," as noted in the APS study, and the necessary beam quality benchmarks have not yet been achieved experimentally.

A. General Considerations

The principal reason that good beam quality is required is to assure good linear gain at the front of the FEL, and this in turn requires a tight resonance between the axial velocity of the electrons and the phase velocity of the FEL ponderomotive wave. If this resonance is tight enough, then all of the

electrons will participate in a "fluid" interaction with the wave, and the exponential wavegrowth rate will occur in the "strong pump" limit for which the growth rate scales as $I_b^{1/3}$ (where I_b is the beam current). However, if the axial velocity spread of the electrons is too great, then the FEL interaction will occur in the "kinetic" regime for which only a subgroup of resonant electrons will drive the wavegrowth. Then the growth rate will scale linearly with I_b and will be much lower. The reduction in linear gain can be devastating to the FEL performance. In the case of oscillator operation, a reduction in gain may mean that the oscillator will fail to start. In the case of amplifier operation, weak linear gain implies a much longer wiggler before trapping can occur, which then increases the vulnerability of the FEL to disruption from growth of sideband modes. A poor quality beam also causes the power spectrum to be broadened, and may lead to incomplete trapping of electrons in the ponderomotive well (i.e., only the resonant electrons become trapped) at the end of the constant parameter portion of the wiggler. This leads to reduced energy transfer from the beam to the laser signal during the nonlinear power amplification in the final tapered portion of the wiggler. (It is normally not possible to avoid a constant parameter wiggler section of linear wave growth at the front end of a high power amplifier, since the nonlinear trapping tends to require laser power of some GW for TW class electron beams, and seed lasers at the GW level with the required pulse time are generally unavailable.)

It is also very important to realize that even when the beam quality is high enough to meet the above requirements for a fluid FEL interaction, the linear and nonlinear gain may still be strong functions of the beam emittance because the beam radius (and hence the current density) is a function of the beam emittance. This arises from the fact that, in the energy and current parameter range for SDI FELs, the wiggler length must be many times the space charge "blow-up" length, necessitating beam focusing in the FEL. The types of focusing commonly envisioned, such as

(i) linear wiggler focusing in one plane, plus quadupole focusing in the other,

(ii) helical wiggler focusing, or

(iii) linear wiggler focusing with curved pole pieces [Ref. 2],

all entail electron trajectories in which the fast wiggler fluctuations are superimposed upon slower "betatron" fluctuations, as illustrated in Figure 1. The hottest electrons (i.e., those with the highest transverse energy) execute excursions in transverse coordinate space which carry them from the beam axis to its edge during a betatron oscillation. The radial size r_b of the beam is then related to the normalized beam emittance ε_n as $\varepsilon_n = \gamma k_\beta r_b^2$, where k_β is the focusing betatron wave number (e.g., $k_\beta \simeq eB_w/\sqrt{2}\ \gamma mc^2$ for helical wiggler focusing where B_w

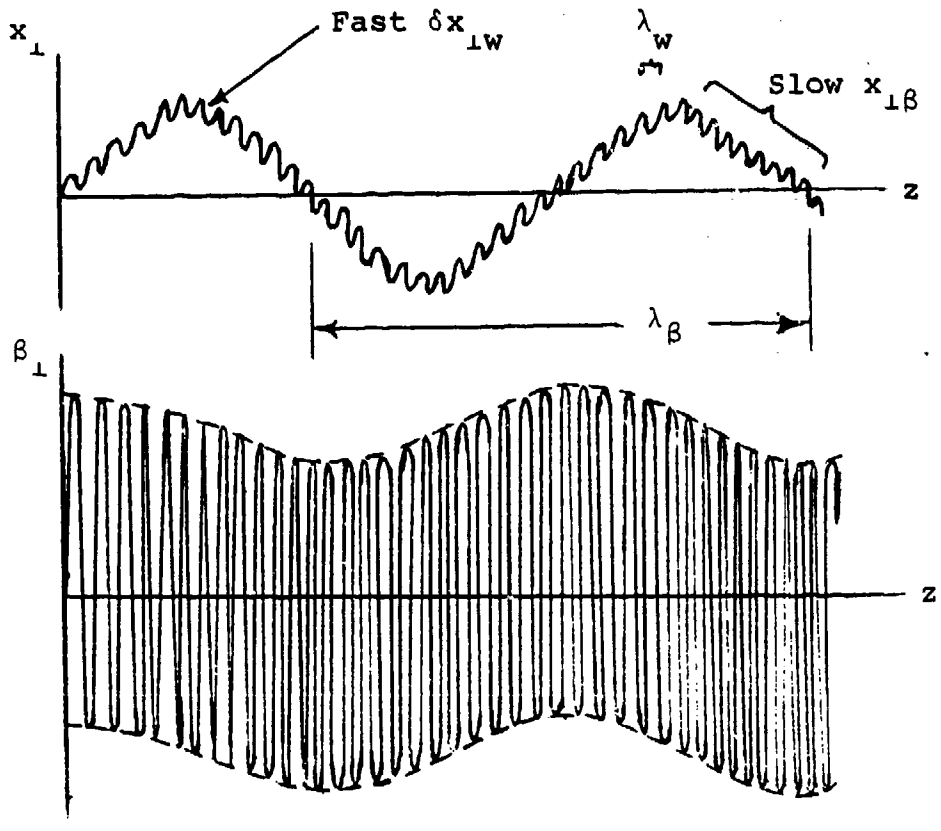

Figure 1. Electron wiggler & betatron oscillations.

is the wiggler magnetic field strength). Because of this relationship, as the beam emittance delivered by the accelerator is reduced, the beam size in the wiggler will be reduced, the linear and nonlinear gain will increase, and it becomes possible for the overall device to become much more compact (and hence less expensive).

In addition to low emittance, it is also important in the design of high power FELs to to push towards high beam current. There are several reasons for this: First is the elementary conclusion that for a given energy extraction efficiency, output laser power increases with increasing beam current. Second, the linear and nonlinear gain are each increasing functions of the beam current [i.e., linear gain $\propto (I_b/\varepsilon_n)^{1/3}$ in the cold fluid regime]. One sees that if a fluid FEL interaction can be obtained, and if ε_n increases less rapidly than linearly with I_b, then linear fluid gain should increase for higher beam current and the required size of the FEL should diminish. Third, the energy given up by the electrons upon trapping, $\Delta\gamma_T mc^2$, also is proportional to $(I_b/\varepsilon_n)^{1/3}$; and hence the saturated laser power level at the end of linear power amplification will scale as $I_b^{4/3}/\varepsilon_n^{1/3}$. One sees that if a fluid FEL interaction can be obtained, and if ε_n increases less rapidly than I_b^4, then the level of saturated laser power following linear gain should increase at higher currents. This is desirable since it diminishes the amount of nonlinear gain which must be obtained in the tapered portion of the wiggler. Finally, in high power FEL

amplifiers, the tapered wiggler section often exceeds the Rayleigh diffraction length. If unconstrained, such diffraccion would cripple FEL operation. Fortunately, these diffraction effects are mitigated by the tendency of the photons to be "optically guided" by their interaction with the electron beam. This optical guiding (whose demonstration is also considered a "critical issue" in the APS study [Ref. 1]) is roughly effective when

$$\frac{a_s}{a_w} = \frac{A_s}{A_w} < \frac{2\nu}{\gamma}$$

where A_s, A_w are the vector potentials of the laser and wiggler fields, $a_s = (eA_s/mc^2)$, $a_w = (eA_w/mc^2) = (eB_w/k_w mc^2)$, k_w is the wiggler wave number, $(\gamma - 1)mc^2$ is the electron kinetic energy, and $\nu = I_b/(\beta_z\, mc^3/e)$ is the Budker parameter. The normalized laser signal strength a_s in turn varies approximately as

$$a_s \approx \frac{2}{k_s r_b} \left(f_T \nu \Delta\gamma \right)^{\frac{1}{2}} \propto \frac{\nu^{\frac{1}{2}}}{\varepsilon_n^{\frac{1}{2}}}$$

where k_s is the optical wave number, r_b is the laser and electron beam radius (presumed roughly equal), f_T is the fraction of trapped electrons, $\Delta\gamma mc^2$ is the energy extracted from these electrons, and the proportionality between r_b and $\varepsilon_n^{\frac{1}{2}}$ has been indicated. From these relations, one may observe that optical guiding requires adequate beam current, and that there is a point of diminishing returns as ε_n and r_b are reduced. At some sufficiently low value of emittance, for a

given beam current, energy, and wiggler parameters, the beam radius will become so small and a_s so large that the photons are no longer guided by such a tight beam. Needless to say, this point of overkill in beam quality improvement is unlikely to be soon reached in the development of a high power FEL for SDI applications.

B. Specific Considerations

As discussed at length in the APS study [Ref. 1], present experimental FEL efforts have been centered around the development of FEL oscillators driven by RF linacs, or around the development of high power FEL amplifiers driven by pulsed induction linacs. Although each approach has its own unique set of technological problems to be solved, the amplifier approach has so far achieved the higher laser power, extraction efficiency, and gain. It is this amplifier approach--utilizing multi-kiloampere beams from an induction accelerator--which is more closely related to our own research on beam handling and emittance control of such high current beams.

The axial velocity resonance which is crucial to the performance of high power FELs is degraded either through increases in the transverse beam emittance (and hence in the transverse velocities), or through increased spreads in the beam energy $\Delta\gamma/\gamma$. Because of the space charge potential of the beam itself, electrons emitted from an equipotential cathode will have an unavoidable radial energy spread of $\Delta\gamma \simeq \nu = I_b/(\beta_z\, mc^3/e)$, where ν is the Budker parameter. However, since

$$\Delta\beta_z \approx \frac{\Delta\gamma}{\beta_z\gamma^3} - \frac{(\Delta\beta_\perp)^2}{2\beta_z} ,$$

the dominant beam quality issue for high energy accelerators will normally be the minimization of transverse velocity spreads (or emittance) rather than energy spreads. [Although it is possible to contemplate FEL designs in which the beam radius is large enough that the $\frac{1}{2}(\Delta\beta_\perp)^2$ term falls below the $\Delta\gamma/\gamma^3$ potential energy spread term, such designs are normally avoided in favor of designs with smaller beams which afford the possibility of a more compact wiggler--both in radial and axial extent.] Since high power FEL amplifier wigglers tend to be a hundred meters in length even for mm-size beams, size constraints are clearly of significant importance.

The normalized emittance of a relativistic electron beam may be approximately defined as $\varepsilon_n = \gamma\beta_\perp r_b = \varepsilon_N/\pi$, where ε_N represents the area of an ellipse in transverse phase space which circumscribes the beam electron coordinates and has intercepts $x_\perp = r_b$, $p_\perp = \gamma\beta_\perp$. (A more precise definition may be formulated as a distribution function-weighted average of the single particle action, as discussed in our paper [Ref. 3] included as Appendix A, and if necessary, the emittance in x,p_x and y,p_y phase space may be separately considered.) The normalized beam brightness may be defined [Refs. 4 and 5] in terms of the normalized emittance as

$$B_n = \frac{2I_b}{\pi^2 \varepsilon_n^2} = \frac{2I_b}{\varepsilon_N^2}$$

(where the factor of two comes from computing the volume of a 4-D ellipsoid in transverse phase space [Ref. 6] as $\frac{1}{2}\pi^2\gamma^2\beta_\perp^2 r^2$.) For a high performance, high power FEL, the beam emittance must be low even at high current, and hence the brightness must also be very high. In the case of a 1μm FEL operating at the high power levels mentioned previously, the APS study estimated [Ref. 7] that a typical "acceptable" emittance is

$$\varepsilon_n = (\varepsilon_N/\pi) < 3 \times 10^{-3} \text{ rad-cm}$$

and that the brightness from an induction linac must be increased to $B_n > 2 \times 10^6$ A/(rad-cm)^2. It was noted in the APS study that induction linacs have yet to achieve these beam quality benchmarks. [It is necessary to insert the caveat that the APS study [Ref. 7] did not make it clear whether the brightness was to be defined as $B_n \equiv 2I_b/(\pi\gamma\beta_\perp r_b)^2$ or as $B_n^* \equiv 2I_b/(\gamma\beta_\perp r_b)^2$. Their parameter ε_N sometimes included the factor of π and sometimes excluded it.]

Indeed, these beam quality criteria may be seen to be rather difficult. With multi-kiloampere beam current, the emittance criteria is the more stringent. Note however that it is necessary in principle that ε_n should be low enough to ensure a fluid, high gain FEL interaction, and that failure to do this may

not be compensated by increasing I_b and hence B_n. The scaling laws considered previously have implied that <u>if a fluid FEL interaction can be obtained</u>, various necessary and desirable performance benefits should accrue from increasing the beam current (provided that ε_n increases less rapidly than I_b). However, the scaling laws are not so favorable for the question which was begged: whether or not a fluid (or strong pump) FEL interaction may be achieved. For helical wiggler focusing, the criterion for a fluid FEL interaction may be roughly expressed as

$$1 \;>\; \frac{k_s^{1/2}\, k_w^{5/6}\, \varepsilon_n^{4/3}}{(1+a_w^2)^{1/2}\, \nu^{1/3}\, F_f^{1/3}} \;\propto\; \frac{\varepsilon_n^{4/3}}{I_b^{1/3}}$$

where F_f is a filling factor to represent the relative photon-electron overlap. One observes that this criterion becomes more difficult at higher current unless the emittance ε_n increases less rapidly than $I_b^{\frac{1}{4}}$. As the $k_s^{\frac{1}{2}}$ factor indicates, this criterion is also more difficult at shorter optical wavelengths. Therefore, it is foolhardy to become sanguine because of the success of lower energy, lower current FEL experiments in achieving a high-gain fluid FEL interaction; the road to successful high energy, high current FEL performance is likely to be rocky.

Generally speaking, it has been found both by ourselves [Refs. 8 and 9] and by others [Refs. 10 and 11], that with some care it is possible to create very high quality electron beams in

relativistic diodes. Indeed, the better quality diode designs afford emittance and brightness parameters which surpass the above-cited benchmark criteria suggested in the APS study. For example, Table I of Reference 10 indicated that the Boeing/MSNW RF LINAC produced a beam with

$$I_b = 0.2 \text{ kA}, \ \varepsilon_b = 10 \text{ MeV}, \ \varepsilon_n = 4.5 \times 10^{-3} \text{ rad-cm} \ ,$$

and hence

$$B_n = 2 \times 10^6 \text{ A/cm}^2\text{-rad}^2$$

(or $B_n^* = 2I_b/\varepsilon_n^2 = 2 \times 10^7$ A/cm^2-rad^2). Table II of Reference 10 reported results of computer simulations which we had performed [Refs. 8 and 9] of high current field-immersed diodes. A diode with high-B_z (i.e., 15 kG) and a smooth foilless anode taper produced a beam with $I_b = 1.2$ kA, $\varepsilon_b = 1.5$ MeV, $\varepsilon_n = 2.85 \times 10^{-3}$ rad-cm, and hence $B_n = 3 \times 10^7$ A/cm^2-rad^2 (or $B_n^* = 3 \times 10^8$ A/cm^2-rad^2).

Barletta, et al. conducted an intensive study [Ref. 11] of diode beam quality, in an effort to improve over the rather poor quality beam obtained in 1985 from the ETA accelerator at LLNL. Often produced from flashboard cathodes and injected through foils, ETA beams were reported [Refs. 11, 12 and 13] with $I_b \simeq 6$-7 kA, $\varepsilon_b \simeq 3.3$-4.5 MeV, $\varepsilon_n \simeq 1.5$-1.8 rad-cm, and hence

$B_n^* \simeq 4\text{-}5 \times 10^3$ A/cm^2-rad^2. (Although the definition of brightness is not included in these cited Livermore references, the numbers quoted in the references are roughly consistent with $B_n^* = 2I/\varepsilon_n^2$.) For use in the ELF amplifier experiments [Refs. 11, 13 and 14], these ETA beams were passed through emittance filters which reduced the current to $I_b \simeq 0.45\text{-}0.85$ kA and produced a normalized edge emittance of $\varepsilon_n \simeq 0.47$ rad-cm. The normalized brightness was roughly unaltered. At $I_b \simeq 0.5$ kA it was reported [Ref. 11] as $B_n^* \simeq 10^4$ A/cm^2-rad^2, and after some improvement in 1986 was reported [Ref. 14] as $B_n^* \simeq 2 \times 10^4$ A/cm^2-rad^2 at $I_b \simeq 0.85$ kA. The brightness of the flashboard cathodes was reported [Ref. 11] in 1985 as $B_n^* \simeq 10^5$ A/cm^2-rad^2. One observes that in 1985 even the flashboard cathode brightness of 10^5 A/cm^2-rad^2 was a factor of 20-200 below the brightness goal of the APS DEW study (depending upon whether one associates the 2×10^6 A/cm^2-rad^2 goal with $B_n = 2I_b/\pi^2\varepsilon_n^2$ or with $B_n^* = 2I_b/\varepsilon_n^2$). The brightness then deteriorated by a further factor of 10 in the ETA accelerator, with the result that even at the 34.6 GHz microwave frequency, a fluid FEL interaction could not be achieved and the linear gain was far below the cold fluid value. In an effort to improve on this situation, Livermore conducted diode design studies [Ref. 11] to obtain improved source brightness. As indicated in Table 1 of Reference 11, a variety of cathodes were estimated theoretically to afford brightness in excess of $B_n^* \simeq 10^7$ A/cm^2-rad^2, including a "controlled field

emission" cathode estimated to produce $I_b \simeq 6$ kA, with $B_n^* \simeq 2 \times 10^8$ A/cm^2-rad^2 and ε_n(inferred) $\simeq 7.8 \times 10^{-3}$ rad-cm. This theoretical normalized source brightness is comparable with the theoretical estimate we had also obtained [Refs. 8 and 9], and is 1 to 2 orders of magnitude above the (post-acceleration) brightness goal of the APS DEW study. Likewise the theoretical normalized source emittance of the Livermore calculations is comparable to that we had obtained, if adjustment is made for the difference in beam current, and these source emittances are comparable with the post-acceleration emittance goal of the APS DEW study.

One may conclude that if realizable in practice, these high-brightness beam sources appear adequate to satisfy even the stringent requirements of beams to drive ground-based FELs for strategic defense applications. However, the looming unsolved problem is how to provide high current beam transport through a very lengthy accelerator in such a manner that emittance growth does not cause the beam quality to deteriorate below the standards required for acceptable FEL performance. On this problem, the experimental results have not been encouraging. Very considerable deterioration in beam quality during beam transport and acceleration has been the rule, not the exception. Furthermore, although source brightness far in excess of the FEL brightness goal is theoretically possible, it appears that there is no room for emittance growth during transport, above the best currently available source emittance, if the FEL emittance goal

of the APS study is to be achieved. (Our own estimates suggest that the APS emittance goal of $\varepsilon_n < 3 \times 10^{-3}$ rad-cm is somewhat conservative--tougher than absolutely necessary--and we take some small reassurance in this possibility.) We perceive the need for considerable advancement in the state of the art of beam quality control during beam transport and acceleration, particularly at high current levels. Our research has been devoted to this problem.

III. REVIEW OF RESEARCH PROGRESS ON BEAM HANDLING AND EMITTANCE CONTROL

In our original proposal [Ref. 15] of November 1985 on beam handling and emittance control, we outlined eight tasks to be performed over a three-year period. When this research was subsequently supported under ONR Contract N00014-86-C-0568 at about 50 percent of the level first proposed, we elected to defer work on Tasks 4, 5, 7 and 8, and we undertook work on Tasks 1, 2, 3 and 6--which were originally stated as follows:

Task 1. Investigate the beam emittance and brightness created in high current, relativistic, field emission diodes. Examine the virtue of shaping the anode-cathode electrodes to minimize emittance. Further examine the virtue of operating the diode magnetic field-immersed, versus a field-free configuration.

Task 2. Investigate the beam emittance gained during the steady state transport of the beam through the accelerator, as the electrons are accelerated to their full energy. Examine the effects of axial acceleration within the accelerating gaps, as well as the effects of axial variations in the focusing forces upon the beam emittance. Compare results of alternative methods of radial focusing and beam transport, including magnetic guiding and channel guiding.

Task 3. Investigate the time-dependent (non-steady state) sources of emittance growth in a channel-guided electron beam due to interactions between the beam electrons and the channel ions or neutrals.

Task 6. Investigate the effectiveness of aperturing the outer beam electrons as a technique of improving the quality of the transmitted beam, and evaluate the tradeoffs of this aperturing approach.

As the research proceeded, we quickly came to the conclusion that the beam quality achievable in magnetic field immersed diodes was quite high, that the emittance growth due to streaming interactions between beam electrons and channel ions appeared likely to be modest, but that there was great danger of large emittance growth during acceleration across gaps or during aperturing. Consequently, we focused most of our research efforts upon Tasks 2 and 6. Furthermore, during the process of reviewing the strengths and weaknesses of alternative transport mechanisms, we reached the tentative conclusion that continuous solenoidal magnetic focusing appeared to offer significant advantages for emittance control during transport and acceleration, in comparison with the gas focusing being exploited in the Livermore experimental program. These advantages derive from the superior experimental control over and tuneability of the magnetic focusing forces. Moreover, it appeared to us that the solenoidal field strength required to limit beam disruption

by the beam breakup (BBU) instability was not excessive, and that the magnetic focusing strength could be reasonably made comparable to the gas focusing strength--at least for beam enery up to a few hundred MeV. Finally, it appeared to us that there was a reasonable prospect that the perceived incompatibility of solenoidal magnetic focusing with FEL operation was illusory, and might be circumvented. Therefore, we placed the primary thrust of our research on determining the efficacy of solenoidal magnetic transport for high current, high quality beams. A secondary goal has been the determination of whether it is preferable to transport beams from shielded or field-immersed cathodes. In what follows we will review the considerations which led us to this concentration on solenoidal magnetic transport, and then we will discuss briefly the highlights of our work in this area. These have been documented more fully in a recent paper [Ref. 3] included herein as Appendix A.

Our analysis of the beam quality achievable in field emission diode sources began with a review of previous work [Refs. 8, 9 and 16] we had conducted in this area. In the preceding Section II, we described a documented [Refs. 8, 9 and 10] design of a smoothly-shaped cathode with a gently tapered foilless anode, immersed in a rather strong (i.e., 15 kG) solenoidal magnetic field. This design yielded a high current beam of extremely high quality: I_b = 1.2 kA, ε_b = 1.5 MeV, $\varepsilon_n = 2.85 \times 10^{-3}$ rad-cm, $B_n = 3 \times 10^7$ A/cm^2-rad^2 (or $B_n^* = 2I_b/\varepsilon_n^2 = 3 \times 10^8$ A/cm^2-rad^2). Another design of an

even higher current foilless diode is illustrated in Figures 2 and 3. These figures demonstrate the beam quality improvements to be gained by replacing sharp corners by gentle tapering of the anode wall. It is also demonstrated that the anode wall may be flared out downstream of the minimum anode radius without causing appreciable emittance growth. The hot, shank-emitted electrons are eliminated by the anode aperture. This diode was immersed in a weaker solenoidal field (i.e., 6.5 kG) and produced a higher ν/γ beam (i.e., $\nu/\gamma \simeq 0.16$), so the beam quality did not approach the earlier-mentioned values; however, the design confirmed the wisdom of gentle electrode shaping.

Meanwhile, other researchers were also conducting research on the beam quality available from diodes, with results which we considered encouraging. For example, Y. Y. Lau [Ref. 17] explored the effects of cathode roughness on the quality of electron beams. He found that roughness-induced beam emittance may be reduced a factor of 2 to 5, if the cathode is operated in the space-charge-limited regime rather than in the temperature-limited regime. His expression for the space-charge-limited roughness-induced beam emittance may be expressed as

$$\varepsilon_n/r_b = \gamma\beta_\perp \simeq 1.22\,(\gamma_o - 1)\left(\frac{h}{d}\right)^{2/3}\frac{h^{\frac{1}{2}}}{(h^2+w^2)^{\frac{1}{4}}}$$

where h,w are the height and width of a cathode bump, d is the anode-cathode gap spacing, and $(\gamma_o - 1)mc^2$ is the diode energy.

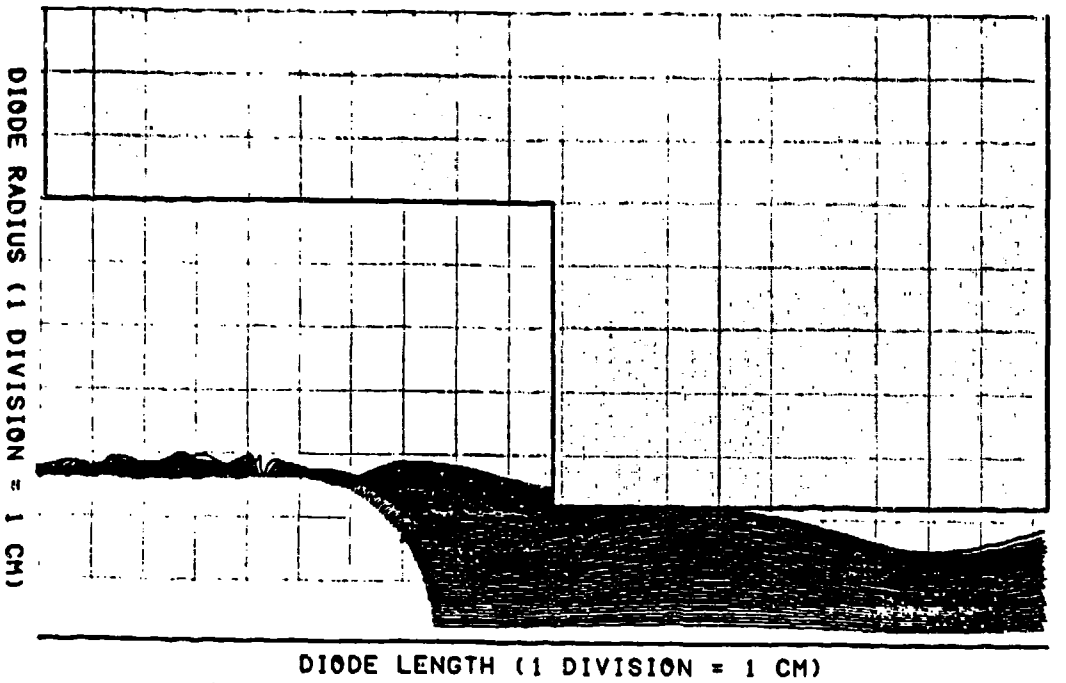

2.3 MV 11 KA 6.0 = BMAX(KG) 22 rad-mm = ε_n

(a) Square Anode Aperture

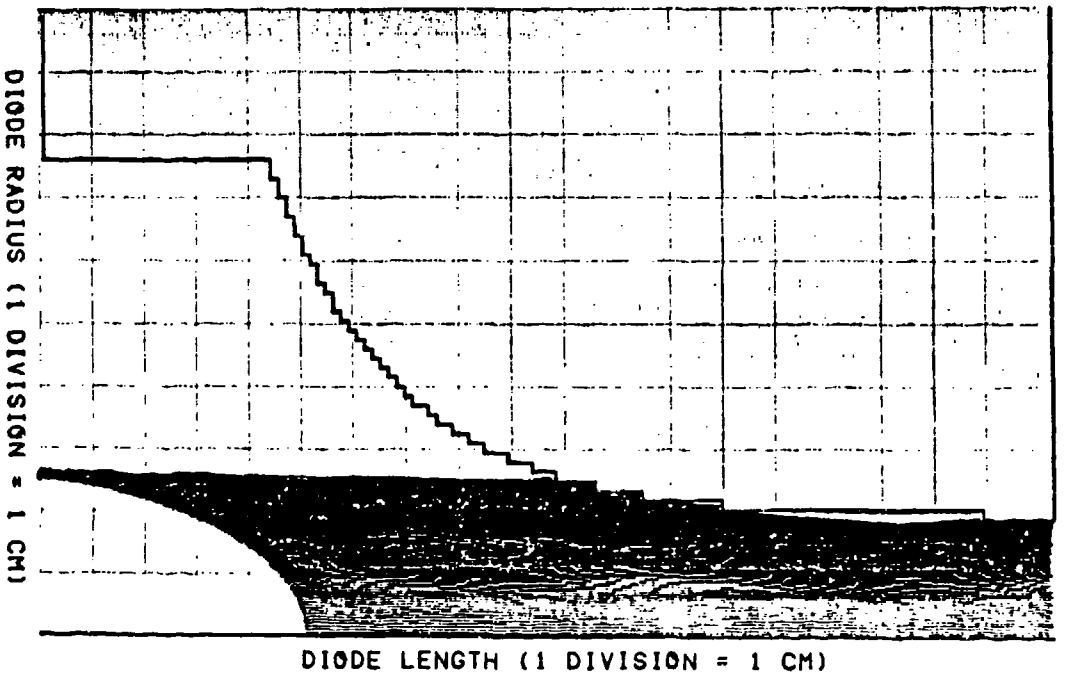

2.3 MV 12 kA 6.5 = BMAX(KG) 5.6 rad-mm = ε_n

(b) Exponentially Tapered Anode Aperture

Figure 2. An illustration of the improvement in beam quality which was achieved for a high current field emission diode by exponentially tapering the anode aperture.

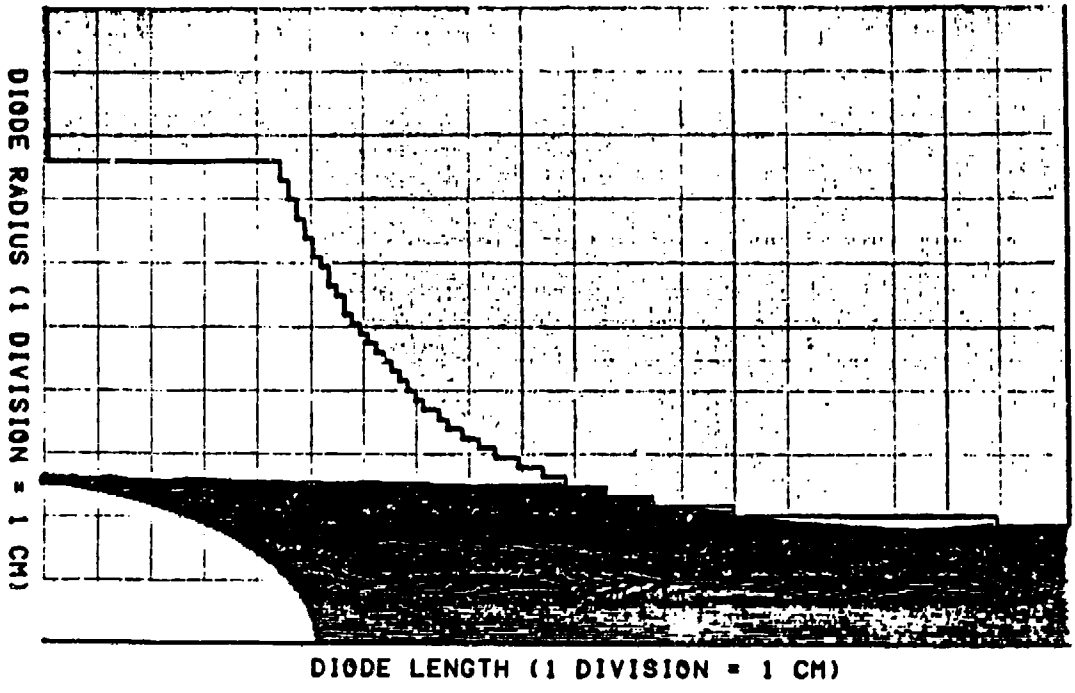

2.3 MV 12 kA 6.5 = BMAX(KG) 5.6 rad-mm = ε_n

(b) Exponentially Tapered Anode Aperture

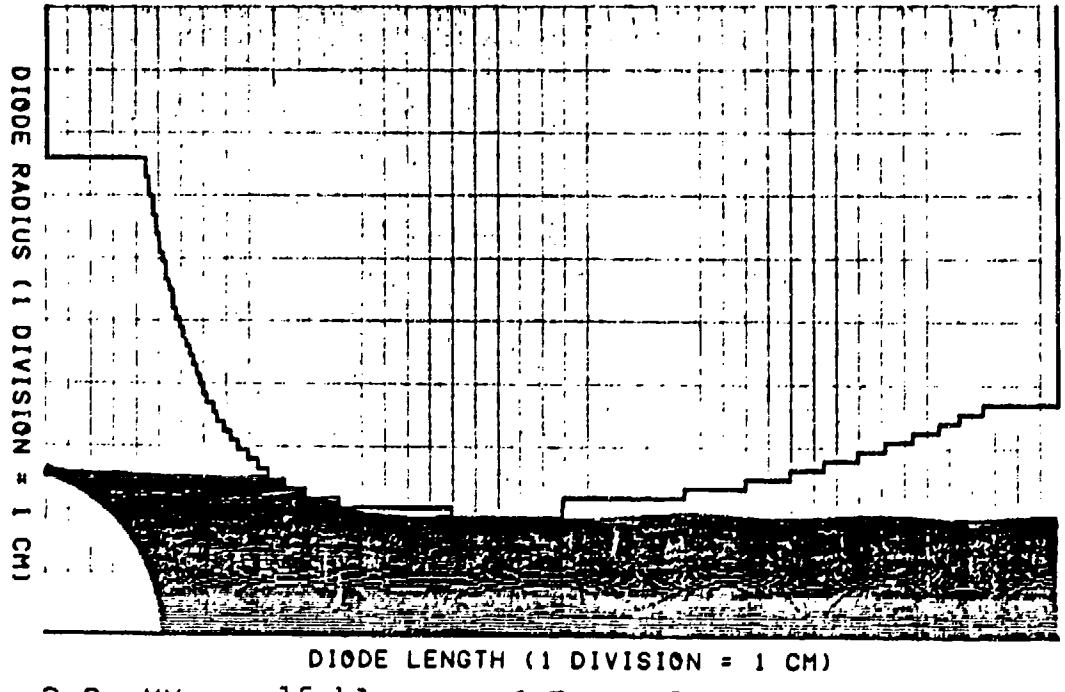

2.3 MV 15 kA 6.5 = BMAX(KG) 5.9 rad-mm = ε_n

(c) Tapered Anode Aperture, with Smooth Flaring

Figure 3. An illustration that the beam quality achieved for a high current field emission diode by smoothly tapering the anode aperture down, may be retained if the anode is later smoothly flared out.

Here one might expect that $h/w \sim \mathcal{O}(1)$ but h/d is quite small, perhaps $\sim 10^{-3}$; space-charge-limited diodes can extract a few kA at 1-2 MeV diode energy, in a beam of radius $r_b < 0.5$ cm. Hence it is quite plausible that the roughness-induced emittance could be held below $\varepsilon_n < 10^{-2}$ rad-cm, and with some effort might approach 10^{-3} rad-cm.

In a similar vein, we examined the emittance induced by passing a beam through an anode mesh of high transparency (i.e., wire dimensions << mesh grid spacing ≡ b). We obtained the result

$$\varepsilon_n / r_b = \gamma\beta_\perp \approx \frac{1}{2\sqrt{6}} \left(\frac{\gamma_o - 1}{\beta_o} \right) \frac{b}{d}$$

which again implies very low emittance beams if b/d is only a few percent.

Finally, there was the cathode emittance study (cited earlier) of Barletta, et al. [Ref. 11], which concluded that with some care multi-kA injectors could be produced with brightness as high as $B_n^* \sim 10^7$ A/cm^2-rad^2. Controlled field emission designs suggested normalized emittance might be held below $\varepsilon_n < 10^{-2}$ rad-cm^2 even for beam current of $I_b \sim 5$ kA.

On the basis of these optimistic results regarding the prospects for high diode beam quality, we decided to defer further intensive diode studies, so as to concentrate on the more dangerous prospect of large emittance growth during beam

transport and acceleration. We do hold the reservation that emittance growth as the beam nears the anode appears somewhat more easily suppressed in immersed cathode diodes than in shielded cathode diodes. However, good success in designing high current shielded cathodes has been reported by several authors [Refs. 11 and 18].

Our preliminary research on Task 3, concerning emittance growth in a channel-guided (or gas-focused) electron beam due to interactions between the beam electrons and the channel ions, also produced results which were optimistic for beam quality. The concept of channel-guided beam transport has been demonstrated at several laboratories, including Lawrence Livermore National Laboratory [Ref. 12]. For channel-guided beam transport, a laser is employed to fractionally ionize a low pressure gas to an ionized density n_i large compared to $\gamma^{-2} n_b$, but small compared to the electron beam density n_b. In this case, the channel electrons are radially expelled by the beam electron self electric field $E_{r/self}$, leaving the massive channel ions behind. Since $n_i > \gamma^{-2} n_b$, the radial electric field of these positive ions will exert a confining force on the beam electrons which exceeds their net space charge forces $-|e|(E_r - \beta_z B_\theta)_{self} \approx -|e| \gamma^{-2} E_{r/self}$. Therefore, the electrons are in effect radially confined by the self-electric field of the ions, and vice versa.

When the electron current lies in the range of 1 kA to 17 kA, the channel electrons are radially expelled on sub-

nanosecond time scales, which is much less than the beam pulse time from an induction accelerator. Subsequently the beam electrons and the channel ions execute radial oscillations in the confining electric fields produced by the space charge of the opposite species; the respective bounce frequencies are $\omega_{Be} = k_G \beta_z c = (2\pi\ n_i\ e^2/\gamma m)^{\frac{1}{2}}$ and $\omega_{Bi} = (2\pi\ n_b\ e^2/M_i)^{\frac{1}{2}}$. (The gas-focusing wave number k_G is sometimes referred to as k_β, and the radial electron oscillations are sometimes referred to as betatron oscillations, which term has assumed a broad generic meaning not restricted to one type of focusing.)

The axial free-streaming energy between the beam electrons and the channel ions is available to drive the growth of streaming instabilities, which are potentially a source of large emittance growth for the beam electrons. Of particular danger are the longitudinal streaming modes, with $k_z \simeq \omega_{bL}/\beta_z c$, where $\omega_{bL} = (4\pi\ n_b\ e^2/\gamma^3 m)^{\frac{1}{2}}$ is the longitudinal beam plasma frequency. These are dangerous because they can produce axial velocity spreading on the beam, which is devastating to the FEL beam quality requirements. However, realizable beam densities are low enough that the longitudinal plasma wavelengths $\lambda_z = 2\pi\ \beta_z c/\omega_{bL}$ exceed a meter at the front of the gas channel, become very much longer as the beam is accelerated, and hence are orders of magnitude larger than the transverse beam dimensions. Consequently, $k_\perp >> k_z$ and the streaming interactions are cast into the transverse regime, where they are likely to culminate in less dangerous transverse beam velocity scatter. Furthermore, the

radial betatron bouncing of the electrons is fast compared to the longitudinal plasma frequency [i.e., $\omega_{Be} > \omega_{bL}$], which produces a reduction in the growth rate of the transverse steaming turbulence by a factor of $(\omega_{bL}/\omega_{Be})^{2/3}$. When the betatron oscillations of the electrons are coherent, at a common frequency, there will be transverse electron "betatron eigenmodes" which are analogous to electron cyclotron modes in a solenoidal field. The transverse streaming interaction will involve a coupling of these electron betatron modes to the ion modes, which will also reflect the radial ion bouncing. The growth rate of the transverse streaming interaction will tend to fall between the two bounce frequencies ω_{Bi} and ω_{Be}. Despite a small fractional neutralization (i.e., $n_i \ll n_b$), ω_{Bi} is often lower than ω_{Be} because of the higher ion mass. (Livermore has employed benzene gas, with molecular weight of 78, in a number of their channel-guided experiments [Refs. 12 and 19].) It appears that for reasonably intense electron beams (e.g., several kA/cm^2), fractional neutralization of 1%-10% benzene ions, and electron energy of a few MeV to several hundred MeV, the linear growth length of the transverse streaming turbulence may be as short as a few meters. In comparison, the accelerator length might be a few hundred meters to produce several hundred MeV beam energy.

Nevertheless, there are several other factors which may mitigate the amount of emittance growth caused by this transverse streaming turbulence. One factor is that the axial wave number

of the fastest-growing transverse modes is tuned to the betatron frequency (i.e., $k_z \simeq \omega_{Be}/\beta_z c$), so that a detuning of the instability occurs as γ is increased. A second factor is that the growth of transverse turbulence can be reduced by design by lowering ω_{Be}, ω_{Bi} or both. However, it is desirable that n_b not be too low in order that the electron beam be a robust driver of the FEL radiation, and it is desirable that n_i not be too low in order that the gas focusing be strong enough to overpower instabilities such as the beam breakup instability (BBU) [Refs. 12 and 19]. It is perhaps possible that heavier gas molecules might be employed, provided that a gas could be found which is suitable for laser photoionization, and otherwise experimentally convenient. Another possibility which has been suggested by Livermore [Ref. 12] and employed by them to some extent is for the gas channel to be somewhat smaller than the beam so that the beam focusing forces are anharmonic and lead to phase-mix damping of coherent transverse beam motion. It has been estimated (Ref. 19] that reasonably small fractional spreads in $k_G = k_\beta$ can lead to complete suppression of the BBU instability, and a similar effect can be expected for the electron-ion streaming instability. Finally, it is expected that the nonlinear result of the transverse streaming turbulence is likely to be the creation of electron (and ion) transverse velocity perturbations, perhaps of magnitude $\delta\beta_{\perp e} \sim k_G r_b$. If so, the streaming-instability-induced emittance growth might be

on the order of a doubling of the incoming normalized emittance, which would likely be tolerable.

Based upon the above considerations, and upon the suspicion that streaming instabilities were not the most threatening technical problem for channel-guided transport, we decided to forego further study of electron-ion streaming turbulence in favor of concentrating on studies of emittance control during beam transport, acceleration, and aperturing. We also decided to focus upon solenoidal magnetic transport, as a tool for the control of emittance growth, despite the perception in some quarters that solenoidal transport might be incompatible with

(1) a multi-cavity high energy accelerator, or

(2) a high performance free electron laser.

Our analysis of these questions of incompatibility is as follows.

The perception that solenoidal focusing might be incompatible with acceleration through a long-multi-cavity accelerator derives from the difficulty experienced by Livermore on the ATA experiments in surmounting problems with the beam breakup (BBU) instability via solenoidal focusing [Ref. 19]. Although the ATA had been designed with solenoidal focusing fields of up to 3 kG, this was determined to be inadequate to avoid unacceptable BBU growth (i.e., the tail of the beam pulse hit the beam pipe), and Livermore had to resort to a somewhat stronger gas focusing. To appreciate the distinction between solenoidal and gas focusing in controlling the BBU amplification,

consider the following amplification formulae cited in Reference 19.

$$\xi_B = \xi_o \exp\left[\frac{I_b}{I_o}\,\omega_o Z_\perp\,\frac{mc^2}{\Delta E_g}\left(\frac{1}{k_c} - \frac{1}{k_{ci}}\right)\right]$$

$$\xi_G = \xi_o \left(\frac{\gamma_i}{\gamma}\right)^{\frac{1}{4}} \exp\left[\frac{I_b}{I_o}\,\omega_o Z_\perp\,\frac{mc^2}{\Delta E_g}\,\frac{1}{2}\left(\frac{1}{k_\beta} - \frac{1}{k_{\beta i}}\right)\right]$$

Here I_b is the beam current, $I_o = mc^3/e \simeq 17$ kA, $\omega_o Z_\perp$ is the product of the angular frequency, the transverse shunt impedance, and the quality factor of the relevant cavity mode, ΔE_g is the change in beam energy per gap, $k_c = eB_z/\gamma mc$ is the cyclotron wave number for solenoidal focusing, $k_\beta = k_G = (2\pi n_i e^2/\gamma\beta_z^2 mc^2)^{\frac{1}{2}}$ is the betatron wave number for gas focusing, k_{ci} and $k_{\beta i}$ are the initial values of these wave numbers, and $(\gamma_i - 1)mc^2$ is the initial kinetic energy of the beam electrons. One may observe that gas focusing benefits slightly from the $(\gamma_i/\gamma)^{\frac{1}{4}}$ factor, representing the radial beam compression which occurs during acceleration of a gas focused beam. There is also an extra factor of $\frac{1}{2}$ in the exponent due to the fact that $k_\beta^{-1} \propto \sqrt{\gamma}$ while $k_c^{-1} \propto \gamma$. (This γ-scaling is a well-known fact of life, which implies that strong solenoidal focusing becomes relatively more difficult at high energy. The other side of that coin is that gas focusing is often relatively more difficult at low energy.) Apart from the two factors mentioned above, the

relative amplifications only differ by the magnitude of the focusing wave numbers. If the Livermore parameters [Ref. 19] (including B_z = 3kG, $n_i = 7 \times 10^{10}/cm^3$, and $\gamma_i \simeq 12.7$ at the 6 MeV onset of gas focusing, $\gamma = 98.9$ at the 50 MeV end of the ATA) are inserted into the above formulae, one finds that the solenoidal focusing allows about 12.7 e-folds while the gas focusing allows only 2.6 e-folds. Although Livermore had earlier touted [Ref. 12] the benefits of the anharmonic phase-mix damping of gas focusing, they concede here [Ref. 19] that "the strength of the channel guiding is so much stronger than that of the solenoids that it is possible to account for nearly all of the BBU reduction without invoking the effects of phase-mix damping." In fact, with the above parameters, k_c varies from 0.30 cm^{-1} to 0.018 cm^{-1} down the accelerator, while k_β varies from 0.15 cm^{-1} to 0.035 cm^{-1}. One finds that the "equivalent solenoidal field strength" for the gas focusing (i.e., such that $k_\beta = k_c$) is 2.14 kG at 6 MeV and 5.95 kG at 50 MeV. Consequently, the 3 kG field available gives superior focusing initially (note that gas focusing was not begun until 6 MeV), but falls short a crucial factor of two by the end of the accelerator. It is apparent that if ATA had the capability to provide 6 kG fields toward the end of the accelerator, and if B_z were increased in $z \propto \gamma^{\frac{1}{2}}$, then the betatron scaling and amplification results could be recovered exactly with solenoidal focusing.

In our judgment, the magnetic field strengths needed for the feasibility of solenoidal focusing are not inordinately high,

even at beam energy levels of several hundred MeV. This is especially true if the payoff is superior beam quality and improved FEL performance. In fact, Livermore paid a price in the degradation of beam quality by resorting to gas focusing. The APS DEW study notes [Ref. 20] that "this approach spoils the beam quality and is not satisfactory for an FEL," and others [Ref. 21] have made the same observation. Other approaches have also been suggested [Ref. 21] to cope with the BBU instability, and solenoidal focusing has been successfully employed on the RADLAC accelerator experiments at Sandia.

The perception that solenoidal focusing is incompatible with the operation of a free electron laser may derive from the difficulty experienced in microwave FEL experiments [Ref. 22] with a solenoidal field present in the wiggler, and from the electron orbit complications [Refs. 23 and 24] which can arise in that circumstance. However, these difficulties primarily arise when the cyclotron wave number k_c is near the wiggler wave number k_w, and in the case of an optical FEL, there will be a vast separation between these wave numbers. Additionally, it is possible to avoid these questions altogether by employing a shielded cathode, introducing a solenoidal field for transport of a beam in Brillouin equilibrium, and then removing the beam prior to injection into the FEL wiggler. This approach has so far been adopted on the RADLAC experiments, and appears to be a viable alternative.

It also seems to us, however, that it may be feasible to employ a field-immersed cathode, to enjoy the beam quality benefits that may then accrue during transport and acceleration, and to retain the solenoidal field in an FEL wiggler. Consider the question of focusing and emittance matching from the accelerator into the wiggler; suppose that gas focusing were used in the accelerator, and helical wiggler focusing were used in the wiggler. To avoid exciting oscillations about the equilibrium beam radius, the beam radius in the accelerator $[r_{bG} = (\varepsilon_n/\gamma k_G)^{\frac{1}{2}}]$ should be matched to the beam radius in the wiggler $[r_{bw} = (\varepsilon_n/\gamma k_\beta)^{\frac{1}{2}}]$, where ε_n is the normalized beam emittance, $k_G = (2\pi\, n_i\, e^2/\gamma mc^2)^{\frac{1}{2}}$ is the gas focusing wave number, and $k_\beta = k_w a_w/\sqrt{2}\,\gamma = e\, B_w/\sqrt{2}\,\gamma mc^2$ is the betatron wave number for wiggler focusing. In this case, $k_G = k_\beta$ should be the matching condition. In the case of solenoidal focusing, with the B_z field to extend into the wiggler, the matching problem is more complex, and is one we propose herein to examine. However, it seems clear that $k_c \sim k_\beta$ is likely to be true, at least in order of magitude. (Recall that $k_c \sim k_G$ would be needed for equivalent focusing in the accelerator.) It follows that $B_z \sim B_w$, and

$$\frac{k_c}{k_w} \sim \frac{a_w}{\sqrt{2}\,\gamma} << 1 \quad .$$

(Note that even if k_c were up to an order of magnitude larger than k_β in the wiggler, k_c would still be much less than k_w for $a_w/\gamma \lesssim 10^{-2}$.)

However, the resonance condition [Refs. 23 and 24] in the electron wiggler trajectory occurs when $k_c = \beta_z k_w$. When $k_c << \beta_z k_w$, as will be true for an optical FEL, then the wiggler orbits are essentially the same type as for $B_z = 0$, and it has been reported [Refs. 23 and 24] that "stable trajectories with nearly constant axial velocities and relatively large wiggler amplitudes are possible." At high energy, it also follows that $k_c << k_w << k_s$, so there will be a large frequency separation between cyclotron radiation and the optical FEL radiation. Consequently, the difficulties previously experienced [Ref. 22] in that regard will be largely eliminated.

For the above stated reasons, we elected to focus the bulk of our beam quality research on the challenging problems of emittance growth during beam transport, acceleration, and aperturing--as expressed in Tasks 2 and 6. We particularly sought (and seek) to determine the efficacy of solenoidal magnetic transport for high current, high quality beams. A secondary goal is the determination of whether it is preferable to transport beams from shielded or field-immersed cathodes, and hence whether to have a solenoidal field in the wiggler. Since our progress on these two tasks has been largely documented in a recent paper [Ref. 3] included as Appendix A, we shall summarize the results only briefly below. This research concerning

solenoidal magnetic transport has so far been restricted to beams from field-immersed cathodes.

We have been sensitive to the potential for large emittance growth during acceleration and transport, having observed this outcome in previous analyses [Refs. 8, 9 and 25] of both solenoidal magnetic and channel-guided transport in situations where nonadiabatic transitions occurred in the beam forces. In the real world, of course, it is not always possible for all transitions to be perfectly adiabatic, which presents the need for a clever and enlightened beam transport design. We found it helpful in our analysis to distinguish between (1) the growth or amplification of previously existing emittance (generally due to nonadiabatic transitions), and (2) the creation of new emittance upon a previously cold beam by the excitation of fluid envelope oscillations, which subsequently phase mix into a truly thermal emittance. The former situation, which is discussed in the first several pages of our paper [Ref. 3] in Appendix A, is the classical kinetic theoretic framework within which emittance is usually defined and analyzed. Emittance is by definition related to the action variable, and hence is preserved as an adiabatic invariant under gentle changes in the focusing forces. Appealing to these adiabatic invariant constraints, one may derive scaling laws for various relevant quantities such as the beam radius, transverse velocity, density, and the focusing frequency ω_o, as functions of the beam Lorentz factor γ down an adiabatic

accelerator. These well-known results are shown in Table 1 of Appendix A for solenoidal magnetic focusing and for ion focusing. The fact that ω_o declines as γ^{-1} for solenoidal focusing, versus $\gamma^{-\frac{1}{2}}$ for gas focusing, has been cited [Ref. 19] by Livermore as favoring the latter. As previously noted, however, a strategy in which B_z increases as $\gamma^{\frac{1}{2}}$ would render these solenoidal and ion focused scalings equivalent.

We also presented results of the increase in preexisting thermal emittance due to a sudden change in γ or in the focusing frequency ω_o. [Note that $\omega_o/\beta_z c$ is essentially the focusing wave number discussed earlier, such as k_c, k_G, k_β.] The growth in thermal emittance is found to be quadratic in the amount of sudden variation in γ, ω_o. Consequently, small sudden changes can be tolerated, but large sudden changes may cause significant emittance growth.

With these necessary background results in hand, our chief effort under this contract has been to investigate the creation of "new" emittance by the excitation of fluid envelope oscillations. Our analysis indicates that this is likely to be the dominant source of emittance growth during beam transport, particularly at high current levels. The reason is that this source of emittance growth is driven by image charges in the surrounding walls, which are larger for high beam currents. Among the more traumatic events which may induce envelope oscillations are the acceleration of the beam electrons across a gap in the surrounding wall, and the aperturing of electrons by a

partially intersecting wall. We have explored each of these processes in detail, for solenoidal magnetic transport of beams from field-immersed cathodes, both analytically and by two-dimensional, steady state, relativistic computer particle simulations. Many of our results are described in Sections 2.1 and 2.2 of the paper in Appendix A.

We were able to obtain quantitative analytical estimates of the amount of emittance growth to be expected, as a function of the wall shape parameters, the axial gradients, and the strength of the focusing forces. These analytical estimates are corroborated by the results of the computer simulations. By far the most significant results obtained are:

1. An indication of how the acceleration gap and aperture walls might be shaped to minimize emittance growth during beam transport; and

2. An indication of how, for a given wall shape, emittance growth might be further reduced by "tuning" the magnetic field to provide compensatory focusing forces to counteract the unavoidable radial forces from the wall image charges.

This tuneability appears to be a crucial tool in the design of low emittance growth beam transport. We found that in several cases it was practical with realistic coil designs and wall shaping to obtain an order of magnitude reduction in emittance

growth, below that which occurred in "unshaped" and "untuned" designs.

As a prelude to the investigation of intersecting beam apertures, we examined emittance growth caused by non-intersecting protuberances. Because the electric equipotentials of a protuberance slice deeply into the beam, the effect on emittance growth is very similar to that of an intersecting aperture--and yet the mathematics is somewhat simpler. In the paper of Appendix A, the analytical and computational comparisons are presented primarily for the case of protuberances, with only a brief discussion of the extension to intersecting apertures. Figures 4 and 5 illustrate the reduction in emittance growth (by a factor of 3.1) obtained with a gentle--but not magnetically tuned--aperture.

During previous computational analysis [Ref. 9] of complex beam transport, it was observed that the outer beam electrons were often perturbed much more than were the inner electrons. This led us to initially harbor the hope that outer electrons might provide a shielding effect for inner electrons, so that if non-perturbing apertures could be developed, it might be worthwhile to purposely transport "extra" outer electrons to function as a sacrificial shield for the inner electrons. However, our analysis promptly revealed that this hope was misguided: extra outer electrons are in fact absolutely counterproductive, because they induce higher image charge forces which then perturb the inner electrons even more.

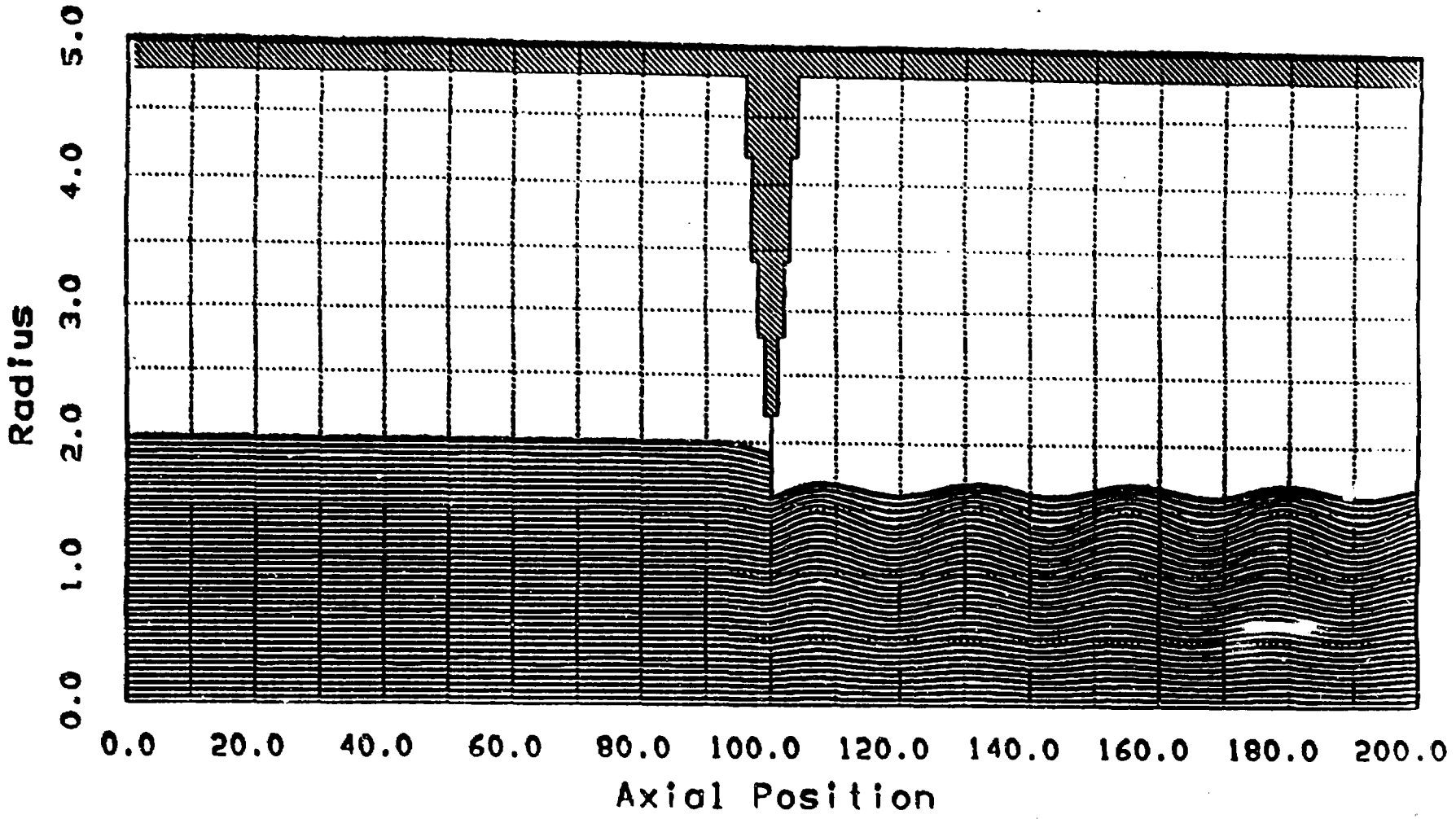

Figure 4. Abrupt aperture (w ≈ 1 cm); $\Delta\varepsilon_n \approx 0.153$ rad-cm.

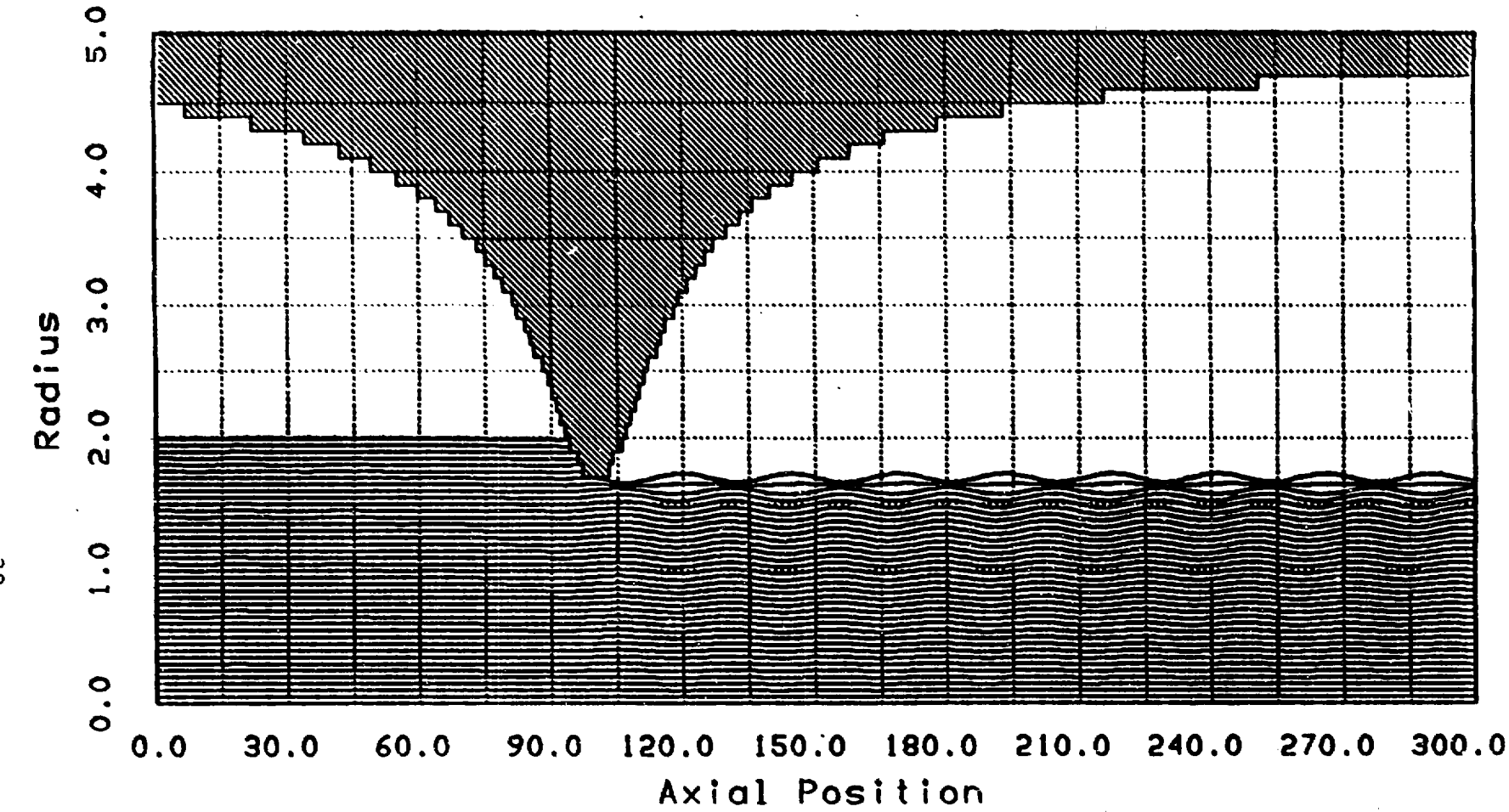

Figure 5. Gentle aperture (w ≈ 10 cm); $\Delta\varepsilon_n \approx 0.049$ rad-cm.

Intersecting apertures are found to have one complicating factor not present in a non-intersecting protuberance: the loss of space charge in the apertured electrons which renders the upstream and downstream beam fields asymmetrical. Because of this feature, advanced aperture designs may benefit from a compensatory asymmetry in the wall shaping.

In the case of both aperture designs and acceleration gap designs, it was found desirable to avoid certain resonance conditions between the cyclotron wavelength $2\pi/k_c$ and the aperture or acceleration gap width. Otherwise the image charge perturbing fields will "drive" the beam near its natural focusing resonance, leading to large emittance growth. Superior beam quality results in the regime of strong focusing/adiabatic gaps (or apertures), for which the cyclotron wavelength is shorter than the axial gap width.

In summary, we have found that beam quality during complex beam transport is enhanced if the walls are shaped to minimize image charge perturbations, if magnetic tuning of the focusing forces is accomplished to compensate for the remnant image charge perturbations, and if the focusing is strong in relation to the gradient lengths of the perturbing forces. We believe these results are both relevant and important to the prospect of achieving the very demanding beam quality goals needed for such SDI objectives as high power, optical free electron lasers.

IV. REFERENCES

1. APS Study: Science and Technology of Directed Energy Weapons, Rev. Mod. Phys. 59, No. 3, Part II, Chapter 3.4 (1987).

2. E. T. Scharleman, J. Appl. Phys. 58, 2154 (1985).

3. J. R. Thompson, M. L. Sloan, B. N. Moore, and J. R. Uglum, "Beam Handling and Emittance Control," Proc. of Innovative Science and Technology Symposium on Microwave and Particle Beam Sources and Propagation, Los Angeles, SPIE 873, 198 (1988).

4. Ref. 1, p. S58.

5. A. Septier. In "Focusing of Charged Particles" (A. Septier, ed.), Vol. II, p. 153, Academic Press, Inc., New York (1967).

6. T. R. Walsh, J. Nucl. Energy, Pt. C, 5, 17 (1963).

7. Ref. 1, p. S58, S61.

8. M. L. Sloan and J. R. Thompson, "A Brief Note on Beam Quality in High Current, Field-Immersed Diodes," Austin Res. Assoc., Rpt. 489 (1983).

9. J. R. Thompson, et. al., "Calculations of the Formation and Transport of High Quality, High Current Relativistic Electron Beams," Austin Res. Assoc., Rpt. I-ARA-86-U-44 (1986).

10. C. W. Roberson, IEEE Jnl. Quantum Elec., QE-21, 860 (1985).

11. W. A. Barletta, et. al., Nucl. Instrum. Methods, Phys. Res. A-239, 47 (1985).

12. W. E. Martin, et. al., Phys. Rev. Lett. 54, 685 (1985).

13. T. J. Orzechowski, et. al., Phys. Rev. Lett. 54, 889 (1985).

14. T. J. Orzechowski, et. al., Phys. Rev. Lett. 57, 2172 (1986).

15. "A Technical Proposal for Analytical Study of Beam Handling and Emittance Control in Advanced Accelerators," Austin Research Associates, Rpt. I-ARA-85-U-64.A (ARA-562), 1985.

16. M. L. Sloan and H. A. Davis, Phys. Fluids 25, 2337 (1982).

17. Y. Y. Lau, J. Appl. Phys. 61 (1), 36 (1987).

18. R. B. Miller, et. al., J. Appl. Phys. 62 (9), 3535 (1987).

19. G. J. Caporaso, et. al., Phys. Rev. Lett. 57, 1591 (1986).

20. Ref. 1, p. S60.

21. R. B. Miller, et. al., J. Appl. Phys. 63(4), 997 (1988).

22. C. W. Robertson, et. al., "A Free Electron Laser Driven by a Long Pulse Induction Linac," Infrared and Milimeter Waves, Vol. 10, ed. by K. J. Button, 361 (Academic Press, 1983).

23. H. P. Freund and A. T. Drobot, Phys. Fluids 25(4), 736 (1982).

24. J. A. Pasour, F. Mako, and C. W. Roberson, J. Appl. Phys. 53(11), 7174 (1982).

25. M. L. Sloan, "Some Considerations on Beam Emittance and Channel Guiding," Appendix B of "Recirculating Accelerator Magnet Design," Final Report, Contract No. 48-1091, Prepared by W. W. Rienstra of Science Applications, Inc. for Sandia National Laboratories (1985).

26. R. C. Davidson, Theory of Nonneutral Plasmas, Chap. 2 (W. A. Benjamin, Inc., Massachusetts, 1974).

27. Ibid, Chap. 1.

28. V. K. Neil, "The Image Displacement Effect in Linear Induction Accelerators," UCID Report 17976 (1978).

29. M. L. Sloan, "A Proposal for Analysis of High Current Beam Instabilities," submitted by Austin Research Associates to Air Force Weapons Laboratory in response to PRDA No. AFCMD82-2, Austin Research Associates Report I-ARA-82-U-57A (ARA-455), 1982.

A P P E N D I X A

J. R. Thompson, M. L. Sloan, B. N. Moore and J. R. Uglum, "Beam Handling and Emittance Control," Proc. of Innovative Science and Technology Symposium on Microwave and Particle Beam Sources and Propagation, Los Angeles, SPIE 873, 198 (1988).

Beam handling and emittance control

J. R. Thompson, M. L. Sloan, B. N. Moore, and J. R. Uglum

Austin Research Associates
1901 Rutland Drive, Austin, Texas 78758

ABSTRACT

A Hamiltonian-theoretic analysis of emittance growth during high current electron beam transport, coupled with an envelope equation analysis of the induced transverse beam oscillations, may be applied to develop scaling laws for the emittance growth suffered during such events as beam acceleration, propagation past irises or constrictions in the waveguide wall, beam aperturing, and axial variation in the magnetic guide field strength. Criteria may be developed for preventing excessive emittance growth by avoiding abrupt axial variations and providing sufficiently strong focusing forces. Designed variations in the waveguide wall shape and in the strength of the magnetic guide field may be introduced to greatly reduce emittance growth during events such as beam acceleration.

1. INTRODUCTION

Advanced electron accelerators will emphasize high current (1 kA or more) concepts that can be scaled to energies of a few hundred megavolts--capabilities which are beyond anything now in existence. As such accelerators are developed, the evolution toward higher currents, higher particle energy, and higher acceleration gradients all conspire to make it more difficult to preserve the necessary beam quality and brightness (i.e., low emittance and energy spread at high current). These requirements are particularly stringent for FEL devices, where to the extent possible all electrons should have the same axial velocity $\beta_z c$ to match the axial phase velocity of the FEL ponderomotive wave.

This axial velocity resonance is degraded either through increases in the transverse beam emittance (and hence in the transverse velocities), or through increased spreads in the beam energy $\Delta\gamma/\gamma$. Because of the space charge potential of the beam itself, electrons emitted from an equipotential cathode will have an unavoidable radial energy spread of $\Delta\gamma \approx \nu = I_b/(\beta_z mc^3/e)$, where ν is the Budker parameter. However, since

$$\Delta\beta_z \approx \frac{\Delta\gamma}{\beta_z\gamma^3} - \frac{(\Delta\beta_\perp)^2}{2\beta_z} \tag{1}$$

the dominant beam quality issue for high energy accelerators will normally be the minimization of transverse velocity spreads (or emittance) rather than energy spreads.

The focusing forces which control the transverse beam dynamics can be described in Hamiltonian formalism, which in many cases assumes the form of a simple relativistic harmonic oscillator

$$H = \frac{1}{2\gamma}\left(p^2 + \frac{\gamma^2\omega_o^2}{c^2} q^2\right) \tag{2}$$

where q is a transverse coordinate, p is the corresponding normalized transverse momentum, and ω_o is the transverse bounce frequency. For such cases, a corresponding action may be defined as

$$J = \oint dq\, p = 2\pi c \frac{H}{\omega_o} \tag{3}$$

and the normalized beam emittance will simply be the average of this action over the transverse phase space (p,q), weighted with the particle distribution function $f(q,p)$

$$\varepsilon_n = \frac{\int dq\, dp\, f(q,p)\, J[H(q,p)]}{\int dq\, dp\, f(q,p)} \,. \tag{4}$$

It is therefore apparent (and well known) that emittance is an adiabatic concept, in the sense that when the focusing forces (e.g., γ, ω_0, hence H) vary only slowly or adiabatically down the accelerator, the action J and normalized emittance ε_n will be preserved as adiabatic invariants.

Nevertheless, in the imperfect real world, all changes cannot occur adiabatically and there are numerous sources of possible emittance growth down an accelerator. A certain, generally small, emittance will be created in the beam diode. Further emittance growth may occur during the matching onto or out of a beam transport system, and during non-adiabatic transitions along the transport system. Emittance growth is common during acceleration across high-gradient acceleration gaps, and during transport past high gradient potential variations associated with wall discontinuities or protuberances. In some cases the beam is apertured and this causes emittance growth for the unapertured portion of the beam. For the case of high current accelerators, the high beam space charge requires relatively strong focusing forces, and tends to exacerbate the problem of emittance control. It is desirable that a high current beam transport system be designed with emittance control in mind, and that it retain sufficient flexibility to cope with unavoidable axial gradients in the transverse forces seen by the beam.

Among the possibilities for the beam transport system are conventional electric or magnetic quadrupoles (often used in low current, very high energy accelerators), IFR (ion focused regime) channels,[1] and solenoidal magnetic transport of beams extracted from either field-free or field-immersed cathodes. We have found that this latter system of solenoidal magnetic transport of beams extracted from field-immersed cathodes appears to be suited to the transport of high current electron beams, and offers the advantage of tuneability, which may be exploited in some cases to minimize emittance growth.

2. ANALYSIS OF EMITTANCE AND EMITTANCE GROWTH DURING SOLENOIDAL MAGNETIC TRANSPORT OF BEAMS FROM FIELD-IMMERSED CATHODES

Beam transport design is facilitated by applying well-known techniques[2,3] based upon the analysis of a differential equation which describes the behavior of the beam envelope in terms of the electric and magnetic potentials and their gradients with respect to the axial z coordinate. In keeping with common practice, steady state, azimuthally symmetric beam flow is assumed and the paraxial approximation is invoked. The relativistic radial force equation

$$\frac{d}{dt}\,\gamma\beta_r = -\frac{e}{mc}\,\beta_\phi B_z - \frac{e}{mc}\left(E_r - \beta_z B_\phi\right) + \frac{c\,\beta_\phi^2}{r} \tag{5}$$

may be combined with the azimuthal canonical momentum constant

$$P_\phi = \gamma r \beta_\phi - \frac{eB_z}{mc^2}\,\frac{r^2}{2} \tag{6}$$

to eliminate β_ϕ, and Maxwell's equations may be solved for the beam self-fields E_r and B_ϕ in terms of the beam current density profile to obtain

$$\frac{d}{dt}\,\gamma\beta_r = -\frac{\Omega_0^2 r}{4\gamma c} + \frac{2 I_b c r}{\gamma^2 \beta_z a^2 (mc^3/e)} + \frac{c P_\phi^2}{\gamma r^3} \tag{7}$$

where $\Omega_0 = eB_z/mc$, I_b is the magnitude of the beam current, $mc^3/e = 17$ kA, and a is the outer beam radius. In the spirit of the paraxial approximation, it is presumed that γ, β_z, B_z, and the beam axial current density $J_z = I_b/\pi a^2$ are roughly uniform in r; $P_\phi \propto r^2$; and $\beta_r, \beta_\phi, E_r, B_\phi \propto r$. Then Equation (7) is self-similar, such that if forces are in equilibrium at one radius, they will be in equilibrium throughout the beam.

The significance of having the cathode field-immersed is that P_ϕ may be appreciable and β_ϕ may be quite small, as the beam propagates in a slowly rotating equilibrium.[4] The centrifugal force in Equation (5) is negligible; the small net outward space charge force (with $E_r - \beta_z B_\phi \simeq E_r/\gamma^2$) is balanced by the $\beta_\phi B_z$ force. If such a slowly rotating beam is near a laminar fluid equilibrium, but also has small thermal velocity perturbations with respect to the desired fluid velocities, these velocity perturbations may be examined by perturbing Equation (7) for the thermal single particle motion about the equilibrium. One obtains an equation for the thermal motion which may be described by a Hamiltonian in the form of Equation (2), where $q = \delta r$, $p = \gamma\beta_r = \gamma\delta\dot{r}/c$, and the thermal bounce frequency is

$$\omega_o = \left(\frac{\Omega_o^2}{\gamma^2} - \frac{8\nu c^2}{\gamma^3 a^2} \right)^{\frac{1}{2}} \quad . \tag{8}$$

This thermal bounce frequency will be near the relativistic gyrofrequency Ω_o/γ for slowly rotating equilibria, for which the current corrections are relatively small. (The thermal bounce frequency is sometimes referred to as the vortex frequency.[5]) When γ is constant, as it generally will be during a single cycle of thermal gyration, the perturbed motion obeys $\delta\ddot{r} + \omega_o^2 \delta r = 0$. If the beam thermal distribution function in the phase space $(\delta r, \gamma\delta\dot{r}/c)$ is presumed of the form

$$f(q,p) = A \exp [- H(q,p)/T] \tag{9}$$

then the thermal action of Equation (8) may be combined with this $f(q,p)$ to obtain the corresponding "normalized thermal beam emittance" from Equation (4) as

$$\frac{\varepsilon_n}{\pi} = \frac{2c}{\omega_o} \frac{T}{mc^2} \quad . \tag{10}$$

The corresponding rms coordinate and velocity fluctuations are $\langle \delta r^2 \rangle^{\frac{1}{2}} = (T/m\gamma\omega_o^2)^{\frac{1}{2}}$, $\langle \beta_r^2 \rangle^{\frac{1}{2}} = (T/\gamma mc^2)^{\frac{1}{2}}$. Since δr represents the thermal gyroradius rather than the beam radius, this thermal beam emittance does not correspond to the usual, experimentally measured beam emittance [i.e., $\gamma(\langle \beta_\perp^2 \rangle \langle r^2 \rangle^{\frac{1}{2}})$]. However, the thermal velocity fluctuations $\langle \beta_r^2 \rangle$ are indeed the relevant component of the measured beam emittance, particularly since the transverse fluid equilibrium velocities [i.e., $\langle \beta_\phi(r) \rangle$] are generally negligible for a slowly rotating equilibrium. When oscillations are excited in the beam fluid motion (i.e., envelope oscillations), these will eventually phase mix to add to the above described thermal emittance and $\langle \beta_r^2 \rangle$.

In the context of accelerator transport, it is of interest to examine how the beam thermal parameters scale as γ is increased down the accelerator. In the ideal case in which γ is adiabatically increased, J and ε_n will be adiabatically preserved. In Table 1 the γ-dependences are listed for both solenoidal magnetic transport of slowly rotating beams, and for ion focused transport.

Table 1

γ-Scaling of Thermal Beam Parameters

PARAMETER	SOLENOIDAL MAGNETIC TRANSPORT, WITH IMMERSED CATHODE	ION-FOCUSED TRANSPORT
J, ε_n	Constant	Constant
ω_o, H, T	γ^{-1}	$\gamma^{-\frac{1}{2}}$
$\langle \delta r^2 \rangle^{\frac{1}{2}}, \langle r^2 \rangle^{\frac{1}{2}}$	Constant	$\gamma^{-\frac{1}{4}}$
$\langle \beta_r^2 \rangle, \langle \beta_\perp^2 \rangle$	γ^{-1}	$\gamma^{-3/4}$
n_b	β^{-1}	$\beta^{-1}\gamma^{\frac{1}{2}}$

For ion focused transport, the restoring frequency is $\omega_o \simeq (2\pi n_i e^2/\gamma m)^{\frac{1}{2}}$, where for the purpose of this comparison it is presumed that the density of ions n_i is uniform in radius and in z, and that $n_i >> n_b/\gamma^2$. In contrast to solenoidal magnetic transport, the hottest electrons in an IFR beam will execute excursions which carry them from the edge of the beam to near the beam axis.

During beam transport down the accelerator, emittance growth may occur either due to non-adiabatic variations in γ, ω_o which cause the existing thermal emittance to increase, or else due to excitation of fluid (envelope) oscillations which subsequently phase mix to add incrementally to the thermal emittance. As we shall later see, there are occasions when one may contemplate designing an abrupt variation in ω_o to eliminate previously excited envelope oscillations which would otherwise phase mix into "new" thermal emittance. However, this strategy entails a price to be paid, in that the previously existing thermal emittance must increase whenever ω_o is abruptly changed.

This effect may easily be demonstrated from Equations (2), (3), (4), and (9) as follows. If γ_o, ω_o are abruptly changed to γ_1, ω_1 (while q,p remain constant), then the

value of H for any particle will abruptly change to $H_1 = (1/2\gamma_1)(p^2 + \gamma_1^2 \omega_1^2 q^2/c^2)$ but will remain constant for subsequent motion. The subsequent motion will have an action $J_1 = 2\pi c\, H_1/\omega_1$, which may be used to compute the subsequent thermal emittance in Equation (4). However, because of the conservation of phase space area and of the distribution function, the averages may be performed over the initial coordinates q_o, p_o and $f_o(q_o, p_o)$ to yield immediately

$$\frac{\varepsilon_{n1} - \varepsilon_{no}}{\varepsilon_{no}} = \frac{\left(\gamma_1\omega_1 - \gamma_o\omega_o\right)^2}{2\,\gamma_1\omega_1\,\gamma_o\omega_o} \quad . \tag{11}$$

First consider the case in which γ_o changes abruptly to γ_1, but the solenoidal field strength B_z does not, as might happen in a short accelerating gap. For the case of solenoidal magnetic transport of a slowly rotating beam from an immersed cathode, the thermal bounce frequency is proportional to γ^{-1}, to the extent that the current density corrections in Equation (8) are negligible. This has the important consequence that H is also proportional to γ^{-1} (even for a sudden change in γ), so that the action J and the thermal emittance ε_n will remain invariant. If the small current density corrections in Equation (8) are retained, then small but finite emittance growth results, given by

$$\frac{\varepsilon_{n1} - \varepsilon_{no}}{\varepsilon_{no}} \approx \left(\frac{8\nu c^2}{\gamma_o a^2 \Omega_o^2}\right)^2 \frac{\left(\gamma_1 - \gamma_o\right)^2}{8\gamma_1^2} << \frac{\left(\gamma_1 - \gamma_o\right)^2}{8\gamma_1^2} \quad . \tag{12}$$

This is one way in which solenoidal magnetic transport of slowly rotating beams has an advantage over alternative focusing schemes for which the restoring frequency is not proportional to γ^{-1}. For example, in focusing schemes such as IFR transport, for which ω_o is proportional to $\gamma^{-\frac{1}{2}}$, the emittance growth during sudden acceleration reduces to

$$\left.\frac{\varepsilon_{n1} - \varepsilon_{no}}{\varepsilon_{no}}\right|_{IFR} = \frac{\left(\sqrt{\gamma_1} - \sqrt{\gamma_o}\right)^2}{2\sqrt{\gamma_1\gamma_o}} \approx \frac{\left(\gamma_1 - \gamma_o\right)^2}{8\gamma_1^2} \quad . \tag{13}$$

where the final expression applies for small acceleration (or deceleration).

The favorable result in Equation (12) should not be interpreted to mean that sudden acceleration of solenoidally focused, slowly rotating beams may be performed with impunity. High gradient acceleration gaps often produce radial as well as axial electric fields, and these may produce envelope oscillations which phase mix to increase the thermal emittance.

Next consider the case in which γ remains fixed, but B_z and hence ω_o are suddenly changed. Then Equation (11) reduces to

$$\frac{\varepsilon_{n1} - \varepsilon_{no}}{\varepsilon_{no}} = \frac{\left(\omega_1 - \omega_o\right)^2}{2\omega_1\omega_o} \tag{14}$$

which demonstrates that the prior thermal emittance suffers an unconditional incremental increase whose magnitude varies quadratically with the abrupt change in the restoring frequency. Equation (14) demonstrates the entropy-like character of thermal emittance, and supports the conventional wisdom that a series of small changes leads to much less emittance growth than a single large change. In order to avoid significant thermal emittance growth, the axial variation in ω_o must be sufficiently gentle that

$$1 << \omega_o L/\beta c \tag{15}$$

where L is the axial gradient length. Virtue therefore attaches to strong focusing (i.e., high ω_o). Condition (15) will also be found to apply to gradients in other perturbing forces which may drive envelope oscillations on the beam, if the magnitude of these oscillations is to be small.

As indicated in Table 1, ω_o will tend to diminish down the accelerator as γ increases. Therefore, short gradient perturbations at the end of the accelerator are dangerous. On the other hand, at the front of the accelerator where γ is low and the beam is less stiff, a given perturbation will tend to create larger perturbed velocities

$\beta_L c$. Here nonlinear effects may be more significant and there is greater danger of the breakdown of paraxial behavior, with consequent emittance growth.

If is of interest to note that the ratio of the restoring frequencies for solenoidal magnetic focusing of slowly rotating beams, to ion focusing, is

$$\frac{\omega_{o\,SM}}{\omega_{o\,IFR}} \approx \left(\frac{4n_b}{n_i\gamma^2}\right)^{\frac{1}{2}} \left(\frac{\gamma a^2\Omega_o^2}{8\nu c^2} - 1\right)^{\frac{1}{2}} . \qquad (16)$$

The second factor is always large for a slowly rotating beam equilibrium, while the first factor is bounded between $2/\gamma$ and 2. Hence at the front of the accelerator, the first factor will be of order unity and it is feasible for beams with solenoidal magnetic focusing to have higher restoring frequencies. On the other hand, since $\omega_{o\,SM}$ declines more rapidly with γ than $\omega_{o\,IFR}$, ion focusing may tend to be stronger at the end of the accelerator.

Previous experience in handling high current beams of relativistic electrons suggests that reasonably low emittance beams are often created in the diode (e.g., less than 0.1π rad-cm for kiloampere beams), only to suffer excitation of large envelope oscillations during transport which phase mix to create much larger emittance than existed initially. The study of such fluid envelope oscillations is facilitated by using an "envelope equation"[3,6,7] which describes the axial behavior of the radial beam envelope. This equation may be expressed as

$$0 = \gamma^2\beta^2 r'' + \gamma\gamma' r' + \left(\frac{\gamma\gamma''}{2} + \frac{\Omega_o^2}{4c^2}\right) r - \frac{2I_b}{mc^3/e}\frac{1}{\gamma\beta r} - \frac{\left(P_\phi^2 + \varepsilon_n^2\right)}{r^3} \qquad (17)$$

and employs the previously discussed paraxial approximations. The primes represent derivatives with respect to the axial z coordinate. It is assumed that the axial dependences of $B_z(z)$ and $\gamma(z)$ are known, and this Equation (17) is then to be solved for $r(z)$. Knowledge of γ is equivalent to knowledge of the electric potential Φ since $\gamma - e\Phi/mc^2$ is constant for steady state flow. The Ω_o^2 term represents a portion of the solenoidal magnetic focusing; the I_b term represents the net outward $E_r - \beta_z B_\phi$ force due to the self space charge of the beam; the P_ϕ^2 term represents a portion of the magnetic focusing and the outward centrifugal forces; the ε_n^2 term represents the outward pressure of existing thermal emittance; and the γ'' term represents radial electric fields other than the beam self radial field. For slowly rotating, magnetically focused beams, the net self space charge forces represented by I_b are relatively weak; the greater danger for the excitation of envelope oscillations is posed by the γ'' radial electric fields which may be produced due to protuberances, discontinuities, or accelerating gaps in the waveguide wall. We now consider the application of the envelope equation to two such classes of beam transport design problems.

2.1 Application to transport past wall protuberances, and beam aperturing

As a first example of a transport design problem which is particularly important for high current beams, we consider propagation past wall protuberances (which do not intersect the beam), or past apertures (which do intersect a portion of the beam). Some schemes for the generation of microwaves with high current beams are based upon loading a surrounding waveguide with non-intersecting irises. An understanding of the influence of wall protuberances upon emittance growth is also relevant to the similar effect produced by wall discontinuities. Not infrequently it is found to be desirable to aperture the outer portion of an accelerated beam prior to using the inner portion, sometimes because the outer portion is relatively "hot." It is desirable to understand how best to accomplish such aperturing with the least perturbation of the transmitted beam core. The emittance growth problems posed by protuberances and apertures will be seen to be intimately related, and understanding these problems is essential to the successful design of a high current beam transport system.

Figures 1 and 2 illustrate the similarity between protuberances and apertures, as well as the emittance growth hazards which they pose. In these examples, a radially uniform 2 cm, 2 MeV, 5 kA electron beam in a 2 kG solenoidal magnetic field is in Figure 1 abruptly apertured to 1.6 cm (hence 1.8 kA is removed), and in Figure 2 is transported past an abrupt protuberance which extends to an inner radius of 2.6 cm. Fluid envelope oscillations in r,ϕ are excited near the cyclotron frequency, with velocity perturbations of magnitude $\delta\beta_r \simeq \delta\beta_\phi \simeq 0.022$, 0.020, respectively. Once phase mixing occurs, growth in normalized emittance will be 0.19π, 0.17π rad-cm, respectively. The reason that the effect of the protuberance is so similar to that of the aperture, producing here about 90% of the

perturbation caused by the aperture, is that the perturbed equipotentials in both cases cut deeply into the beam--producing similar perturbing electric fields.

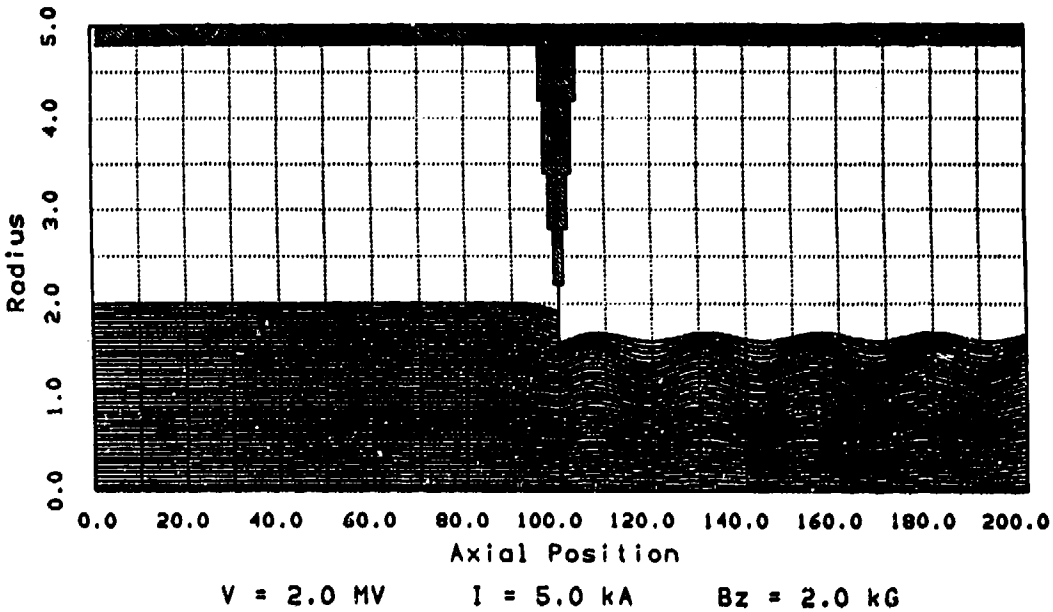

Figure 1. Transport past an abrupt aperature.

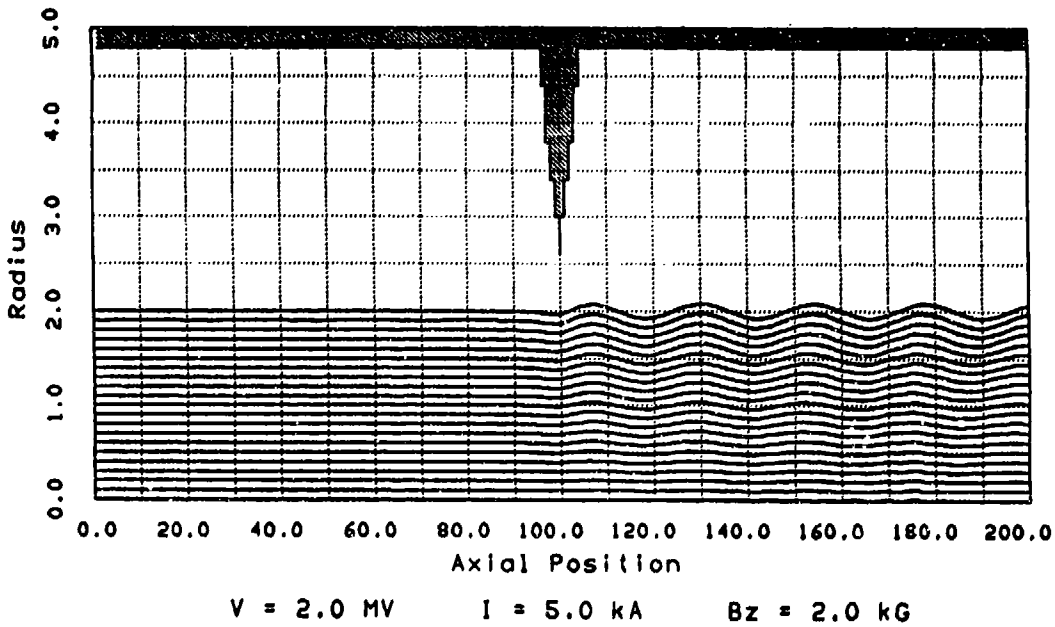

Figure 2. Transport past an abrupt protuberance.

Protuberances, apertures, and wall discontinuities in general are particularly dangerous for high current beam transport, because the perturbing fields are produced by fluctuations in the wall image charge density, whose magnitude is proportional to the beam current. This effect is easily seen analytically by decomposing the total electric potential $\phi(r,z)$ into $\phi_o(r)$ plus $\phi_1(r,z)$, where $\phi_o(r)$ represents the unperturbed beam space charge [i.e., $\nabla_r^2 \phi_o(r) = -4\pi\rho$] and $\phi_1(r,z)$ is the remaining homogeneous part of the potential [i.e., $(\nabla_r^2 + \nabla_z^2)\ \phi_1(r,z) = 0$] needed to satisfy the boundary conditions on a surrounding conducting wall [i.e., $\phi_1(r=b(z),z) = -\phi_o(r=b(z))$]. In the spirit of the paraxial approximation, a power series solution may be developed for $\phi_1(r,z)$ about the beam axis, and the wall boundary condition may be applied with the known space charge potential $\phi_o(r)$, to yield immediately the general solution

$$\frac{e\phi_1(r,z)}{mc^2} = 2\nu \left[\ell n \frac{b_o}{b} - \left(1 - \frac{r^2}{b^2}\right) \left(\frac{bb'' - b'^2}{4}\right) + \ldots \right] \qquad (18)$$

which is valid for wall protuberances of arbitrary profile $b(z)$, so long as the gradients are sufficiently gentle and the beam is not apertured. At large distances from the protuberance it is presumed that $b', b'' \to 0$ and $b(z) \to b_o$ so that ϕ_1 vanishes.

It follows from Equation (18) that the perturbing electric fields which correspond to the wall potential ϕ_1 may be expressed to lowest order as

$$\frac{e E_{1z}}{mc^2} = - \gamma' + \ldots \tag{19}$$

$$\frac{e E_{1r}}{mc^2} = \frac{1}{2} r \gamma'' + \ldots \tag{20}$$

where $\gamma = \gamma_o(r) + 2\nu \ell n\, b_o/b(z) + \ldots = \gamma_o(r) + \delta\gamma(z) + \ldots$ (21)

The r-dependence in $\gamma_o(r)$ has been presumed weak in deriving the envelope Equation (17); the leading z-dependence in γ is seen to come from the wall potential ϕ_1. The perturbing electric fields are directly proportional to the beam current, via the Budker parameter ν. (This already means that it is a bad idea to transport any more current than absolutely necessary, since even the central core of the beam will be perturbed by these image charge fields E_{1z}, E_{1r}.)

As a model, we have considered the symmetric protuberance profile

$$b(z) = b_o \exp\left[- \frac{\Gamma}{\sqrt{1 + (z^2/w^2)}} \right] \tag{22}$$

where w, Γ parameterize the width and depth of the protuberance. The corresponding electron γ-perturbation is

$$\delta\gamma(z) = \frac{2\nu\,\Gamma}{\sqrt{1 + (z^2/w^2)}} \tag{23}$$

and the wall electric fields are the indicated derivatives of this function. It may be seen that the axial electric field E_{1z} points away from the protuberance, while the radial electric field E_{1r} is inward near the protuberance and outward at large distances. This behavior corresponds to image charge which has moved from $z = \pm\infty$ toward the protuberance at $z=0$. Since E_{1z} is larger than E_{1r} and declines less rapidly with z, the beam electrons initially feel a forward acceleration as they approach the protuberance. Only as they come near the protuberance do they feel the radial electric field, which first repels them mildly inward, then pulls them strongly outward as they pass underneath. However, as revealed by the envelope equation, the radial electric field is much more effective at driving transverse perturbations than is the larger axial electric field, which to lowest order merely perturbs the cancellation in the relatively weak $E_{or} - \beta_z B_\phi$ space charge forces.

In order to quantify the amount of transverse beam perturbation induced by a protuberance, it is straightforward to perform a linearized perturbation analysis of the envelope equation. If the beam is presumed to be in a smooth, slowly rotating equilibrium at $z = -\infty$, with $\gamma = \gamma_o$, $r = r_o$, and if the protuberance induces electric fields which perturb $\gamma = \gamma_o + \delta\gamma(z)$, then corresponding radial perturbations $r = r_o + \delta r(z)$ will occur which are described by the linearized envelope equation

$$\delta r'' + k^2\, \delta r = S(z) \tag{24}$$

where

$$k^2 = \frac{\Omega_o^2}{\gamma_o^2 \beta_o^2 c^2} - \frac{4 I_b}{mc^3/e}\, \frac{1}{\gamma_o^3 \beta_o^3 r_o^2} \tag{25}$$

and

$$S(z) = - \frac{r_o}{2\gamma_o \beta_o^2} \left[\delta\gamma'' + \frac{2 I_b}{mc^3/e}\, \frac{1}{\gamma_o^3 \beta_o^3 r_o^2}\, \delta\gamma \right] \tag{26}$$

The envelope oscillations are thus described as a driven harmonic oscillator, with restoring frequency $k \beta_o c = [(\Omega_o^2/\gamma_o^2) - (4\nu c^2/\gamma_o^3 r_o^2)]^{\frac{1}{2}}$ near the relativistic

$$\delta\beta_\perp(z) = \frac{\beta_0}{k}\int_{-\infty}^{z} dz'\, S(z')\, \sin k\,(z - z') \qquad (27)$$

so that

$$\delta\beta_r(z) = \beta_0 \int_{-\infty}^{z} dz'\, S(z')\, \cos k\,(z - z') \quad . \qquad (28)$$

Since our model protuberance of Equations (22) and (23) is symmetric, S(z) is even, and the asymptotic downstream velocity perturbation may be expressed as

$$\delta\beta_r(z) = \left[\beta_0 \int_{-\infty}^{\infty} dz'\, S(z')\, \cos k\, z'\right] \cos k\, z = \delta\beta_\perp \cos k\, z \qquad (29)$$

whose magnitude is simply the Fourier transform of the driving forces in S(z). From Equations (23), (26), and (29), one obtains the result

$$\delta\beta_\perp = \frac{2\nu\,\Gamma}{\gamma_0\beta_0}\left(k^2 - \frac{4\nu}{\gamma_0^3\,\beta_0^2\,r_0^2}\right) r_0\, w\, K_0(kw) \qquad (30)$$

where K_0 is the modified Bessel function of zero order.

For well-magnetized, slowly rotating beams, the k^2 term from the $\delta\gamma''$ radial electric field dominates the $4\nu/\gamma_0^3\beta_0^2 r_0^2$ term from the perturbed self-space charge forces. The coefficient $2\nu\Gamma$ is the peak $\delta\gamma$ acceleration induced by the protuberance. The function $k^2 w K_0(kw)$ is peaked, and falls off exponentially when kw is large. For fixed width w, perturbations maximize @ $k \approx 1.6/w$, and for fixed cyclotron wave number k, the peak occurs @ $w \approx 0.6/k$. These peak responses, of course, correspond to driving the envelope oscillations near the cyclotron resonance [i.e., $w \sim k^{-1}$]. It is clear from the scaling law that the protuberance perturbations should strongly diminish if either B_z or w is increased enough that $kw \gg 1$. Figure 3 illustrates this result, as the beam of Figure 2 is transported past a protuberance with $w \approx 10$ cm, $kw \approx 2.7$. (In comparison, $w \sim 1$ cm for the protuberance shown in Figure 2.) The envelope oscillations induced by the gentle protuberance of Figure 3 are strongly diminished from those induced by the abrupt

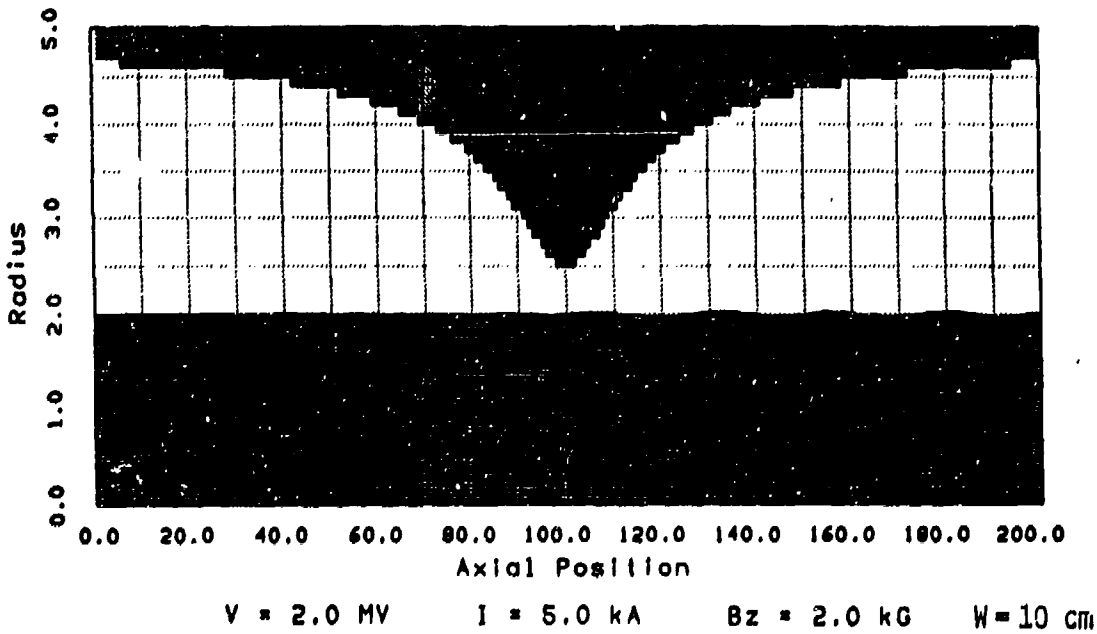

Figure 3. Transport past an adiabatic protuberance.

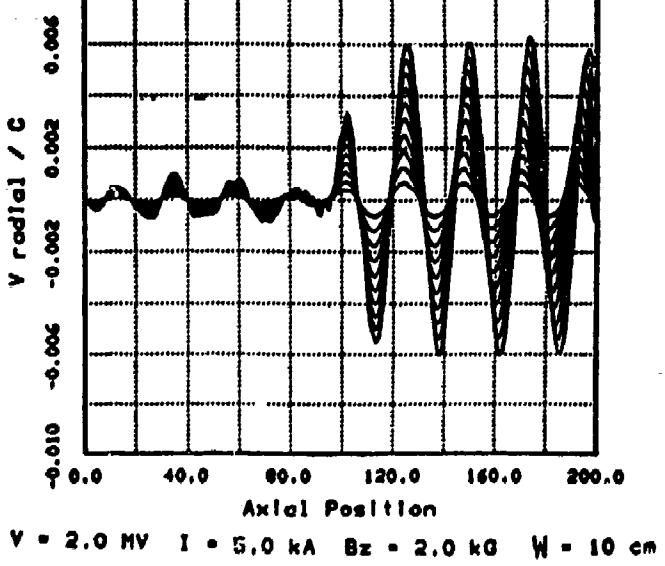

Figure 4. Radial velocity perturbations excited during transport past an adiabatic protuberance.

There are several other methods of reducing the magnitude of excited envelope oscillations, either instead of or in addition to strengthening the magnetic field or making the perturbations more gentle. A conceptually simple method is to design a small abrupt transition in the magnetic field strength, to occur at one of the "waist" positions of the envelope oscillations at a location downstream of the perturbing electric fields (e.g., about 19 cm downstream of the abrupt protuberance of Figure 2). There the radial velocity perturbations will be near zero, and the abrupt magnetic transition should be of a magnitude to reduce the azimuthal velocity perturbations from their peak value to the low value needed for equilibrium propagation. [This desired transition in $\beta_\phi(B_z)$ is easily computed from Equation (6).] There are two principal difficulties with this technique. The first is that for broad perturbations, phase mixing may have already begun to occur before the beam exits the vicinity of the perturbing fields, as may be seen to be the case in Figure 4. The second, more fundamental difficulty is that while an abrupt magnetic transition may "cure" a previously excited envelope oscillation, it is also guaranteed to increase the preexisting thermal emittance in accordance with Equation (14).

A more desirable technique for emittance control, when possible, is to begin with reasonably adiabatic transitions (i.e., $kw > 1$) and then to exploit the tuneability of the focusing magnetic field strength to compensate (i.e., null out) the perturbing forces. The prescription for the compensatory magnetic field shaping is obtainable directly from the envelope Equation (17) by requiring that $r' = r'' = 0$ and that r remain constant. One obtains

$$\frac{B_z^2(z)}{B_z^2(-\infty)} = 1 + \frac{4c^2}{\Omega_o^2(-\infty)\, r_o^2}\left[-\frac{\gamma\gamma''\, r_o^2}{2} + \frac{2I_b}{mc^3/e}\left(\frac{1}{\gamma\beta} - \frac{1}{\gamma_o\beta_o}\right)\right] . \qquad (31)$$

For a strongly focused, slowly rotating beam, the primary correction is for the radial wall electric field represented by $\gamma''(z)$. Where this is largest in magnitude, and negative, underneath the protuberance, B_z should be somewhat increased, and vice versa on the tails of the protuberance. This magnetic shaping was implemented for the adiabatic protuberance of Figure 3, using a least-squares fit routine to select an array of realizable magnetic coils to best achieve the magnetic profile of Equation (31). This results in a further substantial reduction in the induced velocity perturbations from that shown in Figure 4 to the reduced values shown in Figure 5. It is seen that $\delta\beta_\perp$ is reduced to 0.001--a factor of six below that of Figures 3 and 4 (broad protuberance with straight magnetic field) and a factor of twenty below that of Figure 2 (abrupt protuberance with straight magnetic field).

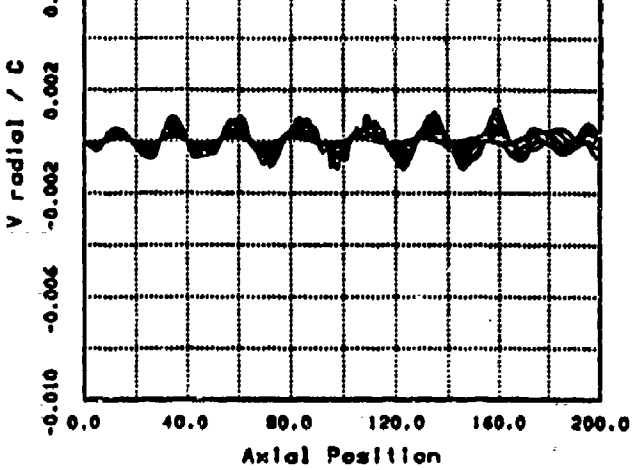

V = 2.0 MV I = 5.0 kA $\overline{Bz}$ = 2.0 kG W = 10 cm

Figure 5. Radial velocity perturbations excited during transport past an adiabatic protuberance, with magnetic compensation.

Extension of these emittance control techniques from the case of a non-beam-intersecting protuberance to a beam-intersecting aperture is straightforward; however, the mathematical functions are more cumbersome. It remains desirable that the aperture width w should be broad in comparison with the inverse cyclotron wave number k^{-1}, in order to minimize the excitation of envelope cyclotron oscillations on the transmitted portion of the beam. It also remains possible to significantly reduce the excitation of envelope oscillations by appropriately shaping the magnetic field through a broad aperture. However, there is one important distinction between a protuberance and an aperture: a symmetric wall profile $b(z)$ will not lead to a symmetric energy perturbation $\delta\gamma(z)$ [or a symmetric radial electric field $E_{1r}(z) \propto \gamma''(z)$] for an aperture in the way that it does for a protuberance. The reason is, of course, that the missing downstream current alters the space charge potential difference between the beam and the conducting wall, in comparison with the value at the corresponding upstream position. It is desirable however that $E_{1r}(z)$ should integrate to give zero average value, and it may prove to be desirable that $\delta\gamma(z)$, $E_{1r}(z)$ be symmetric (although further study of this is needed), in order to realize the low levels of cumulative excitation which are expected for an adiabatic perturbation. Fortunately, this is possible to achieve by designing an asymmetric aperture profile $b(z)$, provided that the fraction of apertured current is not too large. In the case of a beam of uniform current density, the energy perturbation for a gentle aperture may be expressed as

$$\delta\gamma(z) = \nu_0 \left[1 + 2\,\ell n\,\frac{b(-\infty)}{a(-\infty)} - \frac{a^2(z)}{a^2(-\infty)} \left(1 + 2\,\ell n\,\frac{b(z)}{a(z)} \right) \right] \qquad (32)$$

where $b(z)$ is the aperture radius and $a(z)$ is the radius of the outermost electron, which is uniform upstream and downstream, but diminishes during aperturing from $a(-\infty)$ to $a(+\infty)$. Here ν_0 is the Budker parameter for the incoming beam current. [For a protuberance, $a(z)$ is uniform and $\delta\gamma(z)$ reduces to the value in Equation (21)]. Suppose the aperture reaches its minimum radius at $z=0$, with $a(z)$ then known for all z and $b(z)$ known for negative z (i.e., upstream). Then Equation (32) may be used to determine $b(z)$ downstream, such as to produce a symmetric function $\delta\gamma(z)$. This will require pulling the wall away from the beam more rapidly on the downstream side of the aperture than was the case on the upstream side. For example, if $a(+\infty)/a(-\infty) = 0.8$ to aperture 36% of the beam current, and if $b(-\infty)/a(-\infty) = 2$, then $b(+\infty)/a(-\infty) \approx 3.13$. It may also be seen from Equation (32) that in order for E_{1r}, $\gamma''(z)$ to be continuous (hence smooth), $b'(z)$ should vanish at the two points where aperturing begins and ends.

2.2 Application to design of a low emittance, high current accelerating gap

As a second example of a transport design problem which is particularly important for high current beams, we consider propagation through an accelerating gap. Although acceleration per se can lead to an increase in thermal emittance, as indicated in

Equations (12) and (13), the magnitude of such emittance growth is relatively small for a solenoidally focused, slowly rotating beam. Similarly, acceleration per se will perturb the cancellation between the $E_{or} - \beta B_\phi$ self space charge forces (i.e., the $I_b \delta\gamma$ source term in Equation (26)], and thereby excite fluid cyclotron envelope oscillations--but again, the magnitude of these oscillations will be relatively small for a well-focused beam. The greater danger by far, for high current beams, is that large image charge will be induced to collect near an acceleration gap, and this will produce a radial electric field which will strongly excite cyclotron envelope oscillations. (Such accelerating gap-induced oscillations have been previously studied by a number of authors[8,9] in addition to ourselves.)

Such excitation is illustrated in Figure 6, which shows a 2 cm, 2 MeV, 50 kA hollow beam accelerated across a 2 MeV radial gap of 4 cm width and 2.5 cm inner radius.

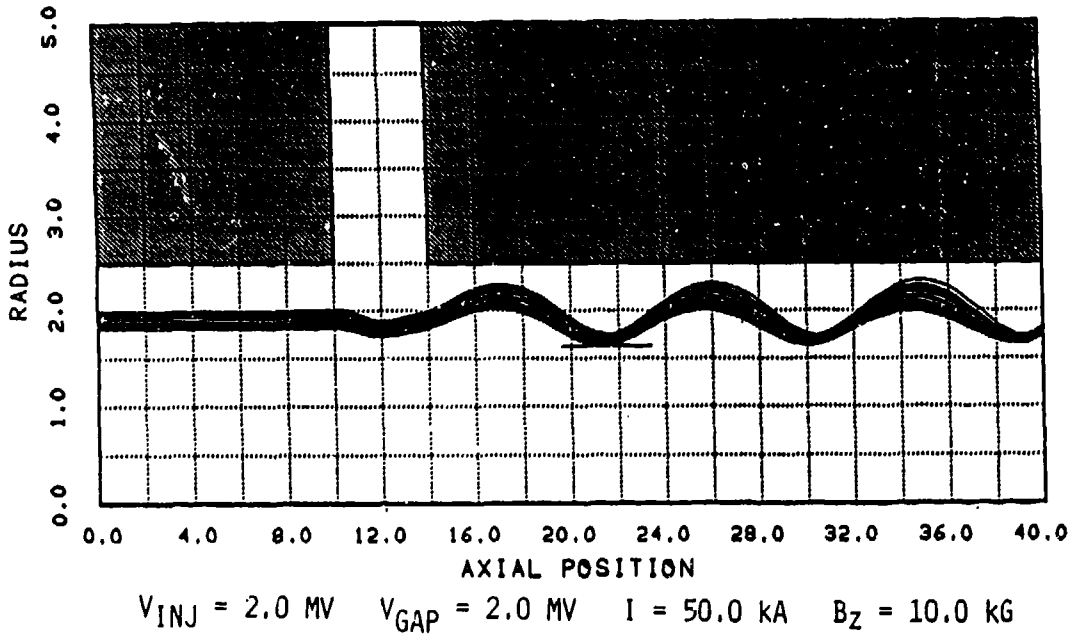

Figure 6. Transport of a very high current hollow beam across a radial feed acceleration gap.

Very strong fluid cyclotron oscillations are excited, and velocity perturbations of $\delta\beta_r \simeq \delta\beta_\phi \simeq 0.21$ are observed, corresponding to a downstream growth in normalized emittance of $3.13\,\pi$ rad-cm. Examination of the equipotential contours for this gap confirms the suspicion that large perturbed radial electric fields associated with image charge near the corners of the gap (particularly the downstream corner) are likely to blame for the beam excitation. Furthermore, this beam has $\nu/\nu_0 \simeq 0.86$ as it enters the acceleration gap, and is therefore rather close to the onset of virtual cathode formation (i.e., "limiting current" phenomena). With this acceleration gap geometry, stable propagation is only possible because of the hollowness of the beam, the nearness of the beam to the wall, and the strong acceleration gradient in the gap which will quickly raise the beam energy to offset the discontinuous increase in the wall radius. However, these features only exacerbate the problem presented by the image charge near the corners of the gap.

A clue to the solution of this problem is the observation from Equations (18) through (20) that a gently varying wall tends to present a "wall electric field" $\vec{E}_1$ which is primarily axial, with a radial component which is smaller by $\sim r/2\ell$, where ℓ is an axial gradient length. The goal may be adopted of seeking to shape the downstream, positive potential wall profile $b(z)$ in such a way that the beam electrons are presented primarily with the DC radial electric field which is present in the upstream flow, plus the accelerating axial electric field in the acceleration gap.

To solve this wall shaping problem, the technique described earlier may be reapplied. The total electric potential $\phi(r,z)$ is decomposed into $\phi_0(r) + \phi_1(r,z)$, where $\phi_0(r)$ generates the self-radial electric field of the beam and $\phi_1(r,z)$ [which obeys $\nabla^2\phi_1(r,z) = 0$] generates the wall electric fields $\vec{E}_1$ --which we again hope to be mainly in the axial direction to represent the accelerating electric field. Let $z=0$ be the beginning of the accelerating gap, where the zero potential wall ends--corresponding to the 10 cm point in Figure 6. For an accelerating gap, the boundary conditions which must be obeyed by $\phi_1(r,z)$ are

where $\Delta\phi$ is the potential jump across the accelerating gap. It has been assumed that the upstream wall remains straight at $b(z<0) = b_o$, and both ϕ_o and ϕ_1 are zero there. The shape of the positive potential downstream wall, $b(z>0)$, is to be solved for. It is presumed that $b(z)$ at least asymptotes to b_o as $z \to \infty$, so that $\phi_1 \to \Delta\phi$ on the downstream wall. Once again a power series solution for $\phi_1(r,z)$ may be developed in the form

$$\phi_1(r,z) = g(z) - \frac{r^2}{4} g''(z) + \ldots \tag{34}$$

valid for r/ℓ small, and the application of the boundary conditions (33) leads to a solution for $\phi_1 = \phi_1[r,b(z)]$ valid for arbitrary downstream wall profiles $b(z)$:

$$\frac{e\phi_1(r,z)}{mc^2} = \begin{cases} 0 & , \ z < 0 \\ \Delta\gamma - 2\nu \left[\ell n \, \dfrac{b(z)}{b_o} + \left(1 - \dfrac{r^2}{b^2}\right)\left(\dfrac{bb'' - b'^2}{4}\right) + \ldots \right] & , \ z > 0 \end{cases} \tag{35}$$

where $\Delta\gamma = e\Delta\Phi/mc^2$.

The best results, in the sense of a weakly perturbing acceleration gap, may be expected if a very gentle wall profile is selected. However, we will demonstrate the power of this technique by showing that very significant reduction in emittance growth is possible with simple functions extending over a finite axial range L. In order to eliminate the large ν-dependent (image charge) wall potential effects, one sees from Equation (35) that $b(z)$ must have the form $b(z) = b_o \exp(F(z)/\nu)$. We selected the model function

$$b(z) = \begin{cases} b_o \exp \dfrac{\Delta\gamma}{4\nu}\left(1 + \cos\dfrac{\pi z}{L}\right) & , \ 0 < z < L \\ b_o & , \ L < z \end{cases} \tag{36}$$

for which the leading z-dependent term in Equation (35) becomes

$$\delta\gamma(z) = \frac{e\phi_1(z)}{mc^2} = \begin{cases} 0 & , \ z < 0 \\ \dfrac{\Delta\gamma}{2}\left(1 - \cos\dfrac{\pi z}{L}\right) & , \ 0 < z < L \\ \Delta\gamma & , \ L < z \end{cases} \tag{37}$$

with E_{1z} and E_{1r} then given in terms of $\delta\gamma(z)$ according to Equations (19) and (20). Since $E_{1r} \simeq -\frac{1}{2} r E_{1z}'$, the radial wall electric fields will indeed be smaller than the axial accelerating field when $\pi r/2L$ is a small parameter.

In order to assess the magnitude of envelope oscillations driven by such an accelerating gap design, a perturbation analysis of the envelope Equation (17) leads again to Equations (24) through (28), with $\delta\gamma(z)$ now given by Equation (37). In this case, the downstream perturbations are found to obey

$$\delta\beta_r(z > L) = \delta\beta_\perp \sin k\left(z - \frac{L}{2}\right) \tag{38}$$

where

$$\delta\beta_\perp = \frac{\Delta\gamma}{2\gamma_o\beta_o} \, k r_o \, \frac{\cos\frac{1}{2}kL}{1 - \frac{k^2L^2}{\pi^2}} \left(1 - \frac{4\nu}{\gamma_o^3 \beta_o^2 k^2 r_o^2}\right) \tag{39}$$

in analogy with the prior result of Equation (30).

$$\phi_1\left[r = b(z), z\right] = \begin{cases} \phi_0\left[r = b(z) = b_0\right] = 0 & , z < 0 \\ \Delta\phi - \phi_0\left[r = b(z)\right] = \Delta\phi + \dfrac{mc^2}{e}\, 2\nu\, \ell n\, \dfrac{b_0}{b(z)} & , z > 0 \end{cases} \tag{33}$$

where $\Delta\phi$ is the potential jump across the accelerating gap. It has been assumed that the upstream wall remains straight at $b(z < 0) = b_0$, and both ϕ_0 and ϕ_1 are zero there. The shape of the positive potential downstream wall, $b(z > 0)$, is to be solved for. It is presumed that $b(z)$ at least asymptotes to b_0 as $z \to \infty$, so that $\phi_1 \to \Delta\phi$ on the downstream wall. Once again a power series solution for $\phi_1(r,z)$ may be developed in the form

$$\phi_1(r,z) = g(z) - \frac{r^2}{4}\, g''(z) + \ldots \tag{34}$$

valid for r/ℓ small, and the application of the boundary conditions (33) leads to a solution for $\phi_1 = \phi_1[r,b(z)]$ valid for arbitrary downstream wall profiles $b(z)$:

$$\frac{e\phi_1(r,z)}{mc^2} = \begin{cases} 0 & , z < 0 \\ \Delta\gamma - 2\nu\left[\ell n\, \dfrac{b(z)}{b_0} + \left(1 - \dfrac{r^2}{b^2}\right)\left(\dfrac{bb'' - b'^2}{4}\right) + \ldots\right] & , z > 0 \end{cases} \tag{35}$$

where $\Delta\gamma = e\Delta\phi/mc^2$.

The best results, in the sense of a weakly perturbing acceleration gap, may be expected if a very gentle wall profile is selected. However, we will demonstrate the power of this technique by showing that very significant reduction in emittance growth is possible with simple functions extending over a finite axial range L. In order to eliminate the large ν-dependent (image charge) wall potential effects, one sees from Equation (35) that $b(z)$ must have the form $b(z) = b_0 \exp(F(z)/\nu)$. We selected the model function

$$b(z) = \begin{cases} b_0 \exp\, \dfrac{\Delta\gamma}{4\nu}\left(1 + \cos\, \dfrac{\pi z}{L}\right) & , 0 < z < L \\ b_0 & , L < z \end{cases} \tag{36}$$

for which the leading z-dependent term in Equation (35) becomes

$$\delta\gamma(z) = \frac{e\phi_1(z)}{mc^2} = \begin{cases} 0 & , z < 0 \\ \dfrac{\Delta\gamma}{2}\left(1 - \cos\, \dfrac{\pi z}{L}\right) & , 0 < z < L \\ \Delta\gamma & , L < z \end{cases} \tag{37}$$

with E_{1z} and E_{1r} then given in terms of $\delta\gamma(z)$ according to Equations (19) and (20). Since $E_{1r} \simeq -\frac{1}{2}\, r\, E_{1z}'$, the radial wall electric fields will indeed be smaller than the axial accelerating field when $\pi r/2L$ is a small parameter.

In order to assess the magnitude of envelope oscillations driven by such an accelerating gap design, a perturbation analysis of the envelope Equation (17) leads again to Equations (24) through (28), with $\delta\gamma(z)$ now given by Equation (37). In this case, the downstream perturbations are found to obey

$$\delta\beta_r(z > L) = \delta\beta_\perp \sin k\left(z - \frac{L}{2}\right) \tag{38}$$

where

$$\delta\beta_\perp = \frac{\Delta\gamma}{2\gamma_0\beta_0}\, k r_0\, \frac{\cos\frac{1}{2}kL}{1 - \frac{k^2L^2}{\pi^2}}\left(1 - \frac{4\nu}{\gamma_0^3\beta_0^2 k^2 r_0^2}\right) \tag{39}$$

in analogy with the prior result of Equation (30).

For fixed cyclotron wave number k, the perturbations maximize at $L=0$, while for fixed L, they maximize at $k = \pi/L$. This corresponds to one-half cyclotron wavelength in the acceleration gap, a resonance at which large perturbations are naturally expected. There are also null responses at $kL/\pi = 3,5,7,...$, although these require longer gaps and nonlinear effects would still produce some excitation. Once again, one expects that the acceleration gap perturbations should strongly diminish if B_z or L is increased enough that $kL/\pi >> 1$ --the adiabatic regime.

From Equation (36), one notes that the maximum positive potential wall radius is $b_{max} = b(0) = b_0 \exp \Delta\gamma/2\nu$. In order for the radial gap size to remain reasonable, it is therefore necessary that $\Delta\gamma \leq \mathcal{O}(\nu)$. Consequently, this sort of gap design is ideal for higher current beams, since larger acceleration gradients are then possible.

Another advantage of this accelerating gap design is that the length L may be increased to restrain the size of $\delta\beta_\perp$, without danger of virtual cathode formation.

In order to test this design, the high current beam of Figure 6 is accelerated through a 2 MeV shaped gap which has been lengthened to $L = 10$ cm, as shown in Figure 7. As the Figures 6 and 7 reveal, a sharp reduction in the perturbation amplitude was indeed

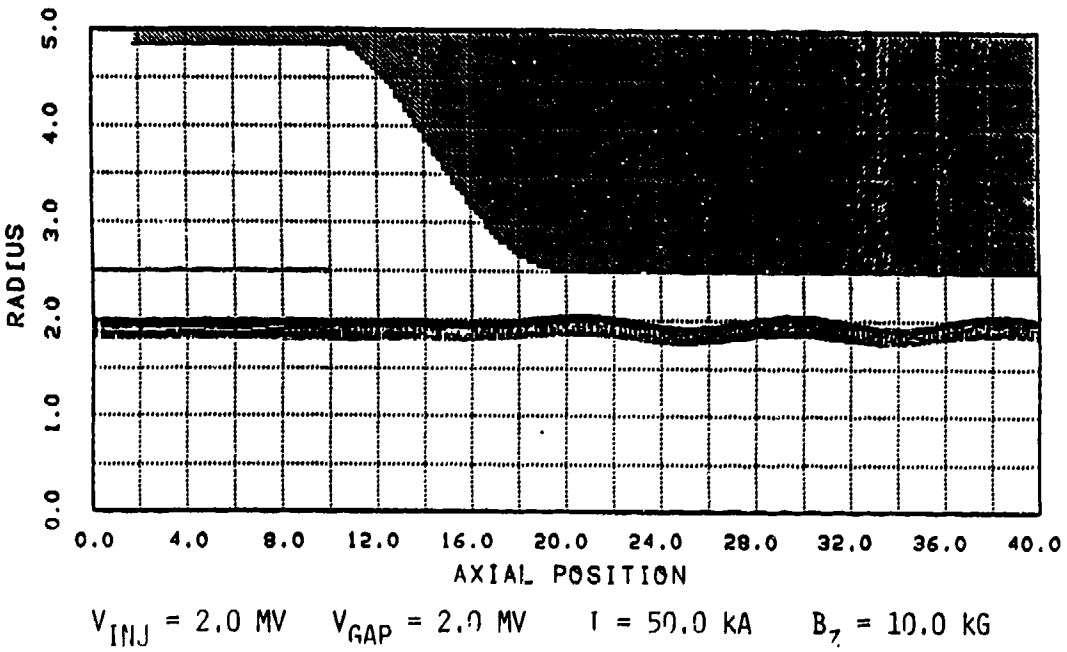

Figure 7. Transport of a very high current hollow beam across a shaped, re-entrant feed acceleration gap.

achieved, with $\delta\beta_\perp$ falling from 0.21 to 0.05. Although one might suspect that the predictions of linearized analysis would be unreliable for a "perturbation" which doubled the beam energy, Equation (39) (with k, γ_0 evaluated in the center of the gap) predicts $\delta\beta_\perp = 0.045$ for the shaped gap. The parameter kL/π varied from 5.4 to 2.5 across this shaped gap, so the adiabatic reductions in emittance growth were expected.

To further test the merit of such shaped accelerating gap designs, a much lower current solid beam of 2 cm, 1 MeV, 5 kA was accelerated across a 0.2 MeV gap. For this beam, ν/γ_0 is only 0.11; hence even a square (or radial) gap could be lengthened to several beam radii without approaching the threshold of virtual cathode formation. Such a conventional radial accelerating gap of 10 cm width is displayed in Figure 8, with beam confinement by a relatively weak 1 kG solenoidal magnetic field. The velocity perturbations excited are displayed in Figure 9, and may be seen to be $\delta\beta_\perp \approx 0.0175$ downstream of the gap. For these parameters, kL/π varies from 0.58 to 0.52 across the gap; hence B_z is so weak that the adiabatic reduction in the perturbations for a corresponding 10 cm shaped gap are not expected. Nevertheless, it is expected that a shaped gap for these parameters would show diminished envelope oscillations due to elimination of the sharp corner in the positive potential wall. Transport through such a gap is shown in Figure 10, which does reveal significantly reduced oscillations. In Figure 11, the velocity perturbations downstream of the gap may be seen to be $\delta\beta_\perp \approx 0.0075$--about 43% of the level with the conventional radial gap.

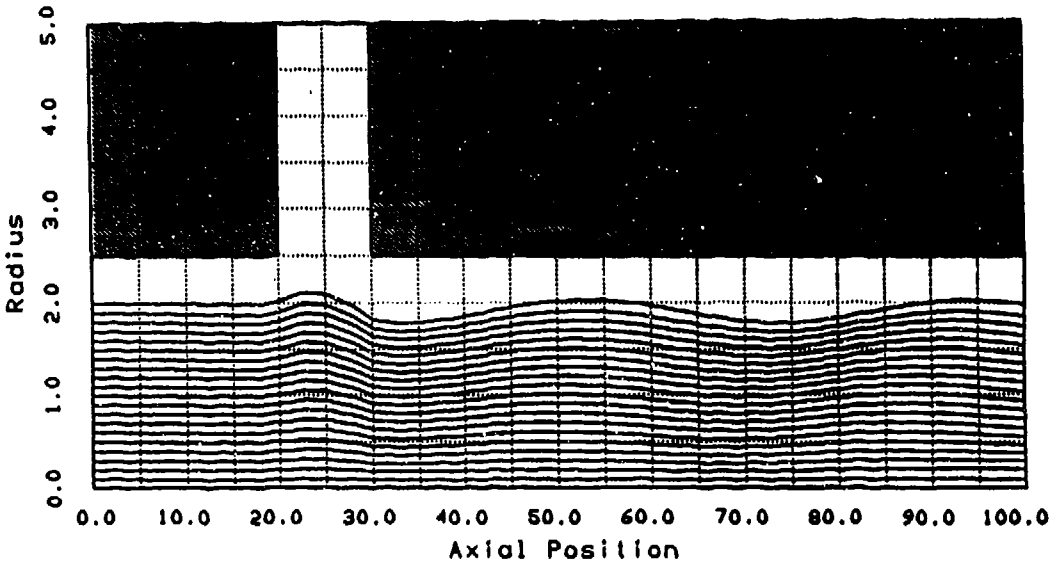

V_{INJ} = 1.0 MV V_{GAP} = 0.2 MV I = 5.0 kA B_z = 1.0 kG

Figure 8. Transport of a high current solid beam across a radial feed acceleration gap.

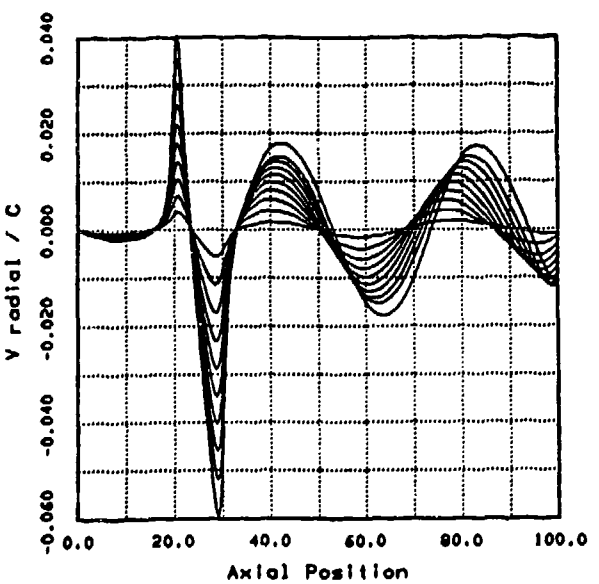

V_{INJ} = 1.0 MV V_{GAP} = 0.2 MV I = 5.0 kA B_z = 1.0 kG

Figure 9. Radial velocity perturbations excited during transport of a high current solid beam across a radial feed acceleration gap.

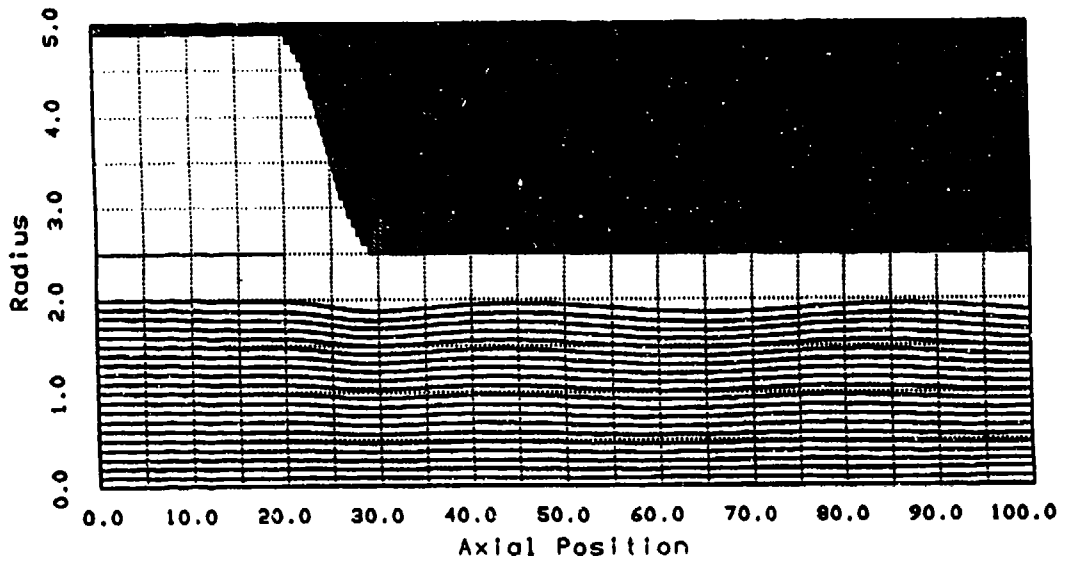

V_{INJ} = 1.0 MV V_{GAP} = 0.2 MV I - 5.0 kA B_z = 1.0 kG

Figure 10. Transport of a high current solid beam across a shaped, re-entrant feed acceleration gap.

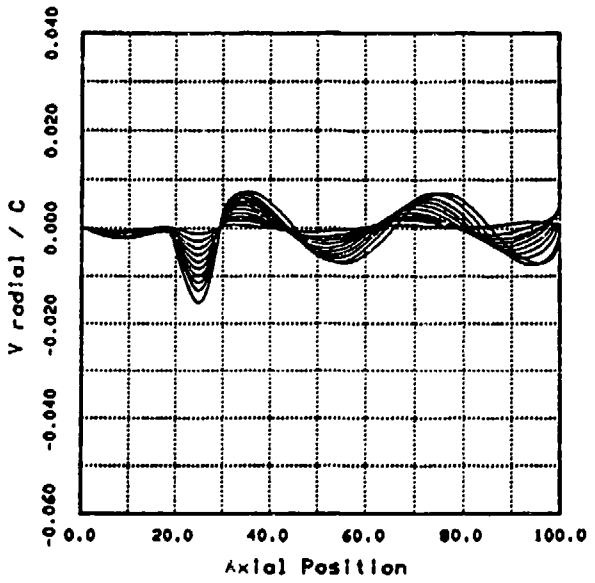

V_{INJ} = 1.0 MV V_{GAP} = 0.2 MV I = 5.0 kA B_z = 1.0 kG

Figure 11. Radial velocity perturbations excited during transport of a high current solid beam across a shaped, re-entrant feed acceleration gap.

Finally, just as in the case of protuberances and apertures, it is possible to attain further reductions in the excitation of envelope oscillations by shaping the magnetic field profile $B_z(z)$ to compensate for the perturbing fields in the accelerating gap. The prescription for the magnetic field profile is again given by Equation (31). This technique was applied to the 50 kA hollow beam accelerated through the shaped acceleration gap of Figure 7. The resulting, further improved beam transport is shown in Figure 12. As before, the magnetic shaping was accomplished with a realistic array of coils. Diagnostics

indicate that the velocity perturbations were reduced to $\delta\beta_\perp \approx 0.0185$: about 37% of the perturbations seen in Figure 7 and less than 9% of the perturbations seen in Figure 6.

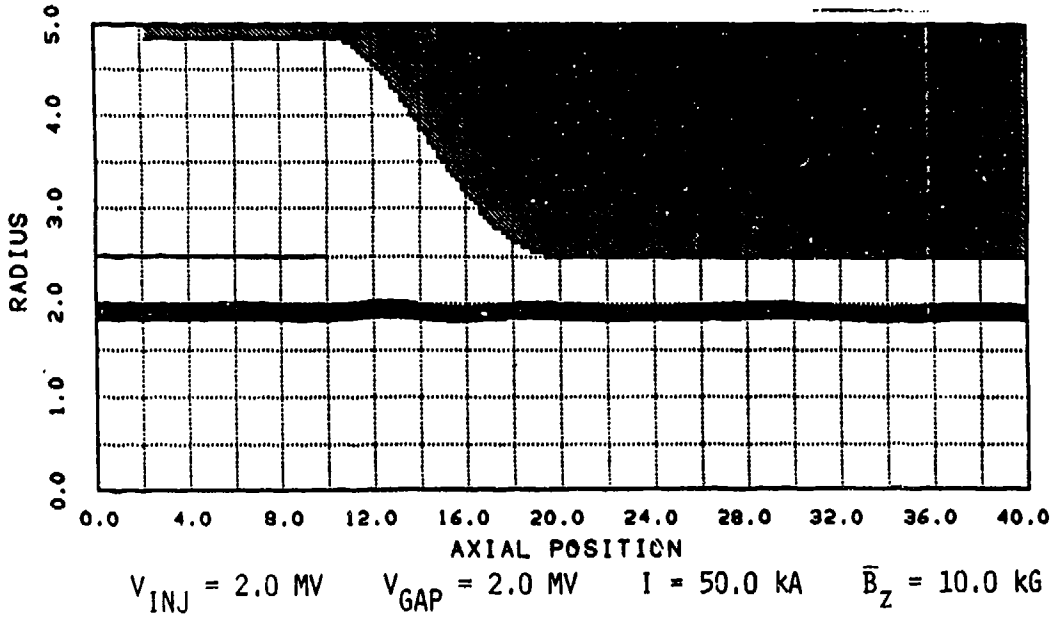

Figure 12. Transport of a very high current hollow beam across a shaped, re-entrant feed acceleration gap, with magnetic compensation.

3. CONCLUSIONS

It has been demonstrated herein that solenoidal magnetic transport of beams extracted from field-immersed cathodes appears to be suited to the transport of high current electron beams. Abrupt wall variations, or protuberances, or abrupt variations in the focusing magnetic field strength are potential sources of growth in thermal emittance as well as in the excitation of envelope oscillations which may phase mix to increase the thermal emittance. Aperturing a portion of the beam without significant emittance growth appears possible, provided that the aperture wall profile is gentle ($kw > 1$) and shaped to account for the current eliminated. High current acceleration gaps can be designed to minimize emittance growth from image charge electric fields by appropriately shaping them. Emittance growth in both apertures and acceleration gaps can be further reduced by shaping the axial profile of the magnetic field to compensate for predictable electric perturbations. This tuneability is one of the significant attributes of solenoidal magnetic focusing.

4. ACKNOWLEDGEMENTS

This research was conducted under ONR Contract N00014-86-C-0568.

5. REFERENCES

1. W. E. Martin, G. J. Caporaso, W. M. Fawley, D. Prosnitz, and A. G. Cole, Phys. Rev. Lett. 54, 685 (1985).
2. P. T. Kirstein, G. S. Kino, and W. E. Waters, Space Charge Flow (McGraw-Hill, New York, 1967), Chap. 3.
3. A. Septier, Applied Charged Particle Optics (Academic Press, New York, 1983).
4. R. C. Davidson, Theory of Nonneutral Plasmas (W. A. Benjamin, Inc., Massachusetts, 1974), Chap. 2.
5. Ibid, Chap. 1.
6. E. P. Lee and R. K. Cooper, Part. Accel. 7, 83 (1976).
7. G. J. Caporaso, A. G. Cole, and J. K. Boyd, IEEE Trans. Nucl. Sci. NS-32, 2605 (1985).
8. T. C. Genoni, M. R. Franz, B. G. Epstein, R. B. Miller, and J. W. Poukey, J. Appl. Phys. 52, 2646 (1981).
9. R. J. Adler, Phys. Fluids 26, 1678 (1983).